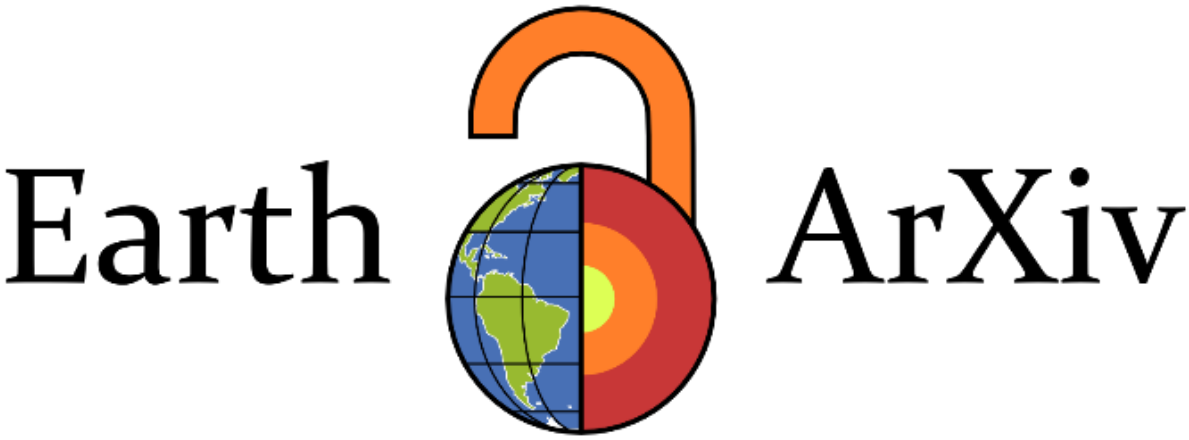

Extreme changes in water level regenerate reed stands and a stable water regime leads to die-off: lessons from the analysis of 40-year satellite times series observations in a shallow lake ecosystem.

Francesco Vuolo[1], Matthieu Collet[1], Rasmus Fensholt[2], Erwin Nemeth[3], Viktor R. Tóth[4]

[1] University of Natural Resources and Life Sciences Vienna, Department of Ecosystem Management, Climate and Biodiversity, Institute of Geomatics, Vienna, Austria
[2] Department of Geoscience and Natural Resource Management, University of Copenhagen, Copenhagen, Denmark
[3] BirdLife Österreich, Vienna, Austria
[4] HUN-REN Balaton Limnological Research Institute, Tihany, Hungary

francesco.vuolo@boku.ac.at
matthieucollet17@gmail.com
rf@ign.ku.dk
erwin.nemeth@birdlife.at
toth.viktor@blki.hu

Abstract

Reed wetlands are key to the productivity of shallow lakes, and their condition is tightly governed by water level variability. Using long-term satellite observations, we provide the first analysis linking hydrology and reed vitality at Lake Neusiedl, a major climate sensitive wetland system in the Pannonian Basin. We assembled a 40-year record (1985–2025) of Landsat derived Enhanced Vegetation Index (EVI) and related it to in-situ measurements of surface water levels to quantify the impact of extreme events. The analyses of hydrological droughts in 1990, 2003 and 2022 (a record low) reveal a decline in plant vitality during periods of low water. Temporary drawdowns are expected to enhance vigour through sediment oxidation and litter decomposition, producing vegetation rebounds as the severity of the drought alleviates. A significant increase in productivity was observed following the 2022 event, but not after the 1990 and 2003 events. The analysis shows that reed vitality is not a continuous linear function of water availability or inundation level. Instead, it follows a pulse-response dynamic, where rejuvenation occurs only when critical thresholds of exposure depth and duration are exceeded, enabling oxidation of accumulated litter and sediment organic matter driving long-term die-back. The results provide a quantitative basis for adaptive water level management at Lake Neusiedl and demonstrate how long-term satellite monitoring can guide reed conservation in shallow lake wetlands more broadly.

1. Introduction

Wetlands are critical ecosystems that provide a wide range of ecological and socio-economic benefits, such as flood regulation, water purification, or carbon storage. Although they cover only about 5–10% of the Earth's land surface (Kingsford et al. 2016), their importance far exceeds their spatial extent. Yet, wetlands are under increasing threat worldwide. Since 1700, at least 21% of global wetlands have been lost (Fluet-Chouinard et al. 2023), mostly due to land conversion for agriculture, urban expansion, industrial development, and aquaculture (Ballut-Dajud et al. 2022; Fluet-Chouinard et al. 2023). These losses have serious consequences, including increased greenhouse gas emissions, diminished water quality, reduced flood protection, and growing risks to biodiversity. In response to these pressures, international frameworks such as the Ramsar Convention have been established to promote the conservation and sustainable management of wetlands (Xu et al. 2019).

In Europe, wetlands are characterised by a broad diversity of ecosystems such as peatlands or fens in northern Europe, floodplain marshes and riparian habitats along major rivers, or coastal wetlands such as saltmarshes and lagoons. The acceleration of drainage and land conversion in the 19th century have contributed to major losses, but the remaining wetlands are now recognised as key providers of ecosystem services, acknowledged in EU policy (Verhoeven 2014; Bertassello et al. 2025). Among these, reed-dominated wetlands formed by stands of *Phragmites australis* are widespread, particularly along lakeshores, river margins, and deltas. Extensive reedbeds occur in major river floodplains and deltas such as the Danube and Rhine, and in the littoral zones of many natural and artificial lakes, where they often form monodominant belts (Čížková et al. 2023). Reeds play a central role in these ecosystems by stabilising shorelines, trapping sediments, and regulating nutrient fluxes, while also providing critical habitat for birds, fish, and invertebrates. At the same time, reed wetlands support socio-economic uses, from traditional thatching material and grazing to waterfowl hunting and fishing, illustrating their dual importance for both nature conservation and local livelihoods (Karstens et al. 2019; Čížková et al. 2023).

A relevant example is the Lake Neusiedl (Neusiedler See/Fertő), an internationally recognised Ramsar site, located on the border between Austria and Hungary. As the westernmost steppe lake in Europe, it represents a unique ecological system (Tolotti et al. 2021). Its expansive reed belt, second in size in Europe after the reed in the Danube Delta (Buchsteiner et al. 2023), provides a vital habitat for a diversity of bird species, making the lake a key site for ornithological conservation. In recent decades, the reed belt has shown signs of ecological decline, with the emergence of the so-called "reed die-back": parts of the reed belt are characterised by reduced vitality, declining biomass, and structural degradation (Nemeth and Dvorak 2022). The causes of reed die-back are multiple and debated, involving poor reed renewal, organic matter accumulation, and hydrological effects. It is known that reed health depends on the balance of wet and dry periods related to surface water level fluctuations. For example, in the Netherlands, (Graveland 1998) described how summer-high, winter-low seasonal water-level fluctuations prevented die-back of the reeds by restricting litter depth and enhancing aeration of the rhizosphere. (van der Putten 1997) similarly recorded the importance of hydrological variation for healthy reed stands.

The exact response is non-linear: on very dry ground reeds lose competition to other species, while on permanently flooded ground reeds suffer from oxygen deprivation. For example, redox measurements at Lake Balaton following the 2003 drought were significantly higher than during periods of high water (Tóth 2016), and this shows greater oxygenation of sediment following drawdown. Together, these local-scale studies demonstrate that alternating wet and dry phases can promote reed vitality. Understanding this interplay and defining a framework for accurate monitoring is especially urgent under ongoing drought trends and resulting, more complex water management decisions for this lake and for similar ecosystems in Europe.

Lake Neusiedl has been described as a "hotspot area of long-term ecological research" (Teubner et al. 2022). Research themes have evolved from 19th-century floristic and faunistic inventories, through biocoenological studies in the 1930s, to species and habitat conservation from the 1960s onwards. More recently, global warming and ecosystem services have come into focus (Teubner et al. 2022). The lake is part of the international Long-Term Ecological Research (LTER) network, highlighting its role as one of the most extensively studied natural systems in Central Europe (LTER Austria, 2025). Monitoring reed belt dynamics at the Lake Neusiedl has long relied on remote sensing. Colour-infrared aerial photography in the 1970s and 1980s provided detailed maps of vitality, density, and height (Csaplovics 1982). Subsequent airborne campaigns and object-based classifications enabled temporal comparisons that revealed shifts in reed structure and the emergence of humic water zones (Csaplovics 2019). Recent drone-based surveys provided high-resolution phenological insights, revealing pronounced vegetation expansion and water retreat under drought conditions (Buchsteiner et al. 2023). The latter study underscored the necessity of scaling observations to broader spatial and temporal extents and emphasized the complementary role of satellite-based monitoring for regional assessment. From our research, we believe that a

comprehensive, regular, and up-to-date representation of temporal and spatial patterns of reed growth dynamics in relation to lake water levels is missing. Specifically:

- There is limited evidence on how extreme hydrological events (droughts and rewetting) affect reed vitality, die-back, and recovery at landscape scale.
- The differential response of reed stands along water depth gradients and edge positions (lakeward vs landward) remains poorly quantified.
- The short-term sensitivity of reed growth to intra-annual water level fluctuations (seasonal monthly changes) is not well characterized.
- A transferable, operational remote sensing framework for continuous reed monitoring that bridges legacy Landsat archives with higher resolution Sentinel-2 data is lacking.

To partially respond to these needs, we have formulated some research questions and addressed them with this study. In particular:

- How did the 2022 hydrological drought and the 2023-2025 rewetting affect reed vitality and spatial patterns of dieback and recovery? Do the previous 1990 and 2003 drought events show comparable impacts and recovery trajectories as in 2022?
- What water depth ranges are associated with reduced vitality, dieback, or regeneration?
- Can we detect recovery in affected areas, and where is recovery most pronounced?
- Are lakeward reed edges more vulnerable to dieback and more responsive to rewetting than landward edges?
- How are water level and air temperature driving reed vitality on a seasonal basis?

This study aims to quantify the temporal and spatial dynamics of reed vitality at Lake Neusiedl over 1985–2025 by integrating Landsat-derived EVI with in-situ surface water level measurements, specifically detecting and mapping die-back and recovery associated with the 2022 droughts and the subsequent rewetting, and assessing how lakeward versus landward stand positions, elevation and water depth modulate these responses. We further seek to characterize short-term sensitivity and long-term resilience by linking monthly water-level and air temperature (using monthly means and anomalies) to EVI-based vitality metrics for different reed functional groups. This second part of the analysis is provided as supplementary materials.

2. Materials and Methods

2.1. Study area

Lake Neusiedl (Neusiedler See/Fertő) is a shallow endorheic steppe lake on the Austria–Hungary border (Figure 1). It is the largest lake in Austria, with a surface area of ~320 km² (77% in Austria), and an average depth of ~120 cm (maximum 180 cm) (Herzig 2014; Tolotti et al. 2021). Water balance is strongly controlled by precipitation and evapotranspiration, which account for ~79% of inputs and 89% of losses (Soja et al. 2013; Sailer and Maracek 2019). Historically, the lake has undergone extreme variability, including a complete dry-out between 1865 and 1870. Water level regulation began in the early 20th century with the construction of the Einser-kanal, followed by hydraulic controls in 1965. Currently the weir of the Einser-kanal is closed until a water level of 115.7 meter above sea level (m a.s.l.) in the winter months and to 115.8 m in the summertime. Yet the system remains highly sensitive to climatic variability (Wolfram et al. 2014). In recent years, drought conditions have been among the most severe on record, and the Einser-kanal weir kept closed since 2015 (Wasserportal Burgenland 2025).

The lake is naturally alkaline and subsaline, with conductivity between 1300–3200 µS cm^{-1} and pH around 8.7 (Buchsteiner et al. 2023). It is recognised for its ecological and cultural importance, being protected as a Ramsar site, Natura 2000 area, transboundary national park, and UNESCO World Heritage cultural landscape (Sailer and Maracek 2019).

Lake Neusiedl hosts one of Europe's largest continuous reed belts (~180 km²), dominated by *Phragmites australis* (117 km² in Austria, 63 km² in Hungary). This reed belt is structurally heterogeneous, ranging from dense stands to degraded zones and open-water patches (Csaplovics and Schmidt 2011). Signs of reed die-back have been observed since the 1990s, particularly along interior zones, raising concerns for biodiversity and management (Nemeth and Dvorak 2022).

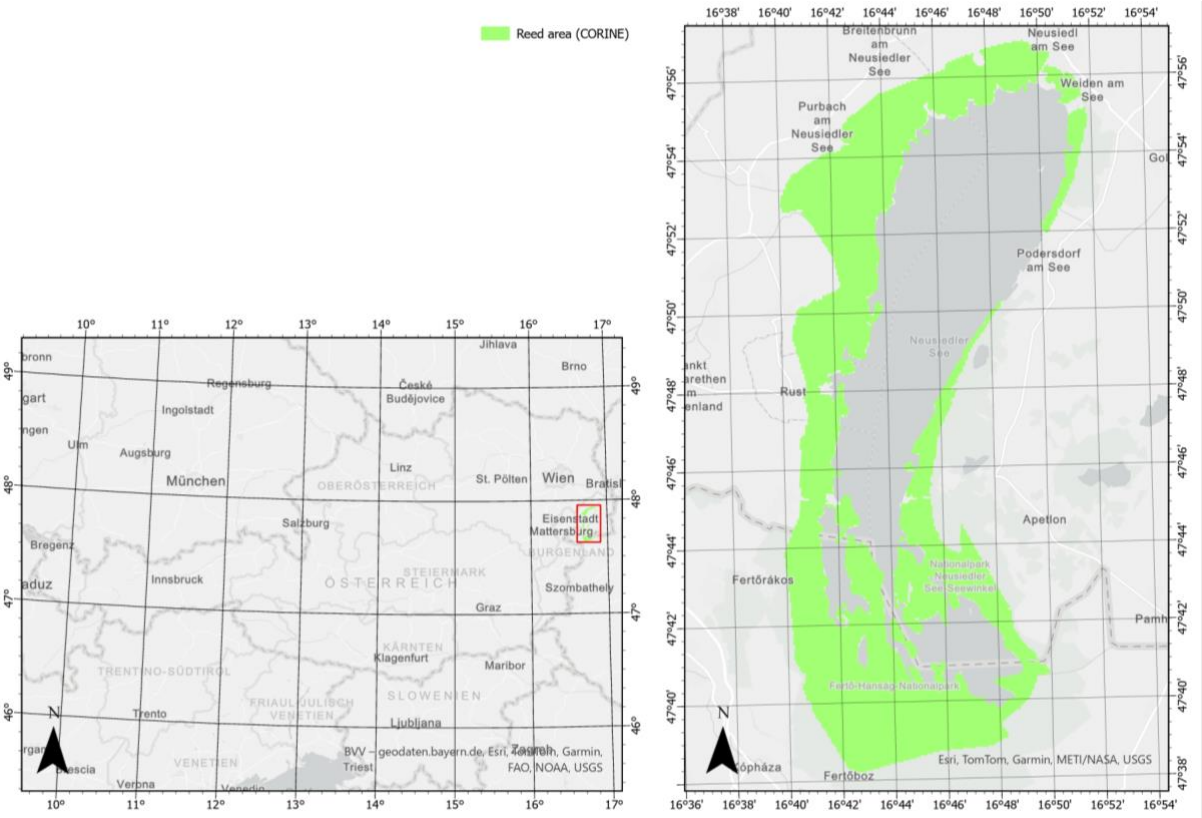

Figure 1 Overview of the study site at Lake Neusiedl, highlighting reed areas (dominated by Phragmites australis) in green. The area is derived from the CORINE Land Cover inventory using class 411 ("Inland marshes") and class 324 ("Transitional woodland-shrub") as they both represent the reed belt.

2.2. Data

2.2.1. Vegetation growth mapping

The data used in this study comprised Earth observation (EO) data, in-situ hydrological data including average surface water level (SWL) and meteorological data (air temperature and precipitation data). In particular, NASA USGS Landsat surface reflectance data based on Collection-2 Level-2 data (that integrates data from multiple satellite missions including Landsat TM, ETM+, OLI, OLI-2) from 1985 to 2025 at 30 m resolution was used to calculate the Enhanced Vegetation Index (EVI) from atmospherically corrected reflectance. The Quality Assurance (QA) masks for clouds, shadows, and snow/ice were applied to flag missing observations. Finally, monthly median values were created for the 40-year period. Some months, especially in the winter period, were missing and filled by linear interpolation between the nearest valid "before/after" observations. This procedure ensured a continuous and spatially coherent EVI time series, suitable for both long-term trend analysis and intra-annual vegetation dynamics.

Other satellite platforms, such as Sentinel-2 allow improved spatial and temporal resolution for monitoring reeds and mapping their distribution, condition and biomass across wetlands (Rupasinghe and Chow-Fraser 2021; Zhao et al. 2022; Baibagyssov et al. 2025). Unfortunately, it is only available from 2015 onwards. In this study, Sentinel-2 data was only used to study the spatial variability of reed growth conditions during the 2022 drought event in the period 2018-2025.

The EVI was selected as the primary indicator for monitoring reed vitality due to its reduced sensitivity to atmospheric interference and soil background effects (Huete et al. 1997). Unlike the Normalised Difference Vegetation Index (NDVI), which saturates in high biomass conditions, EVI maintains sensitivity, preserving information in dense vegetation (Qiu et al. 2018). EVI has demonstrated effectiveness in monitoring *Phragmites australis* and is widely regarded as a reliable proxy for reed vitality, particularly in dense canopy structures (Villa et al. 2013; Serrano-Ortiz et al. 2020). These characteristics make EVI especially suitable for assessing the structure and greenness of the reed belt in Lake Neusiedl.

The extent of the reed belt was obtained from the CORINE (Coordination of Information on the Environment) Land Cover (CLC) dataset from 2018, a European land cover inventory developed by (European Environment Agency 2019). It provides harmonised, high-resolution spatial data on land use and land cover across Europe and classifies land cover into more than 44 thematic categories. Specifically, two classes were included: class 411 ("Inland marshes") and class 324 ("Transitional woodland-shrub"), as both capture the heterogeneous structure of the reed ecosystem in this region. These classes were extracted and combined to form an area of interest specific to reeds, which was used as the spatial boundary for all analyses (Figure 1).

2.2.2. Masking presence of water

Because the presence of water can negatively bias EVI, the log-transformed Vegetation-Adjusted Water Index ($VAWI_{log}$) (Declaro et al. 2025) has been used in an earlier study to detect surface water and the presence of water beneath vegetation and to mask EVI for further analysis. $VAWI_{log}$ performed well in detecting water beneath vegetation; however, the authors indicated that its effectiveness in wetlands and floodplains with vegetation cover required further investigation. Therefore, surface and ground water level measurements (from 1985 to 2025), sediment moisture observations (from 2018 to 2022), and high-spatial-resolution land cover maps (from 2019 and 2022) were used to provide a local verification for the $VAWI_{log}$ threshold used to identify presence/absence of water. A corroboration of the threshold used to detect absence/presence of water was performed using high spatial resolution vector maps for June 2019 and June 2022 identifying three categories including reed, water and sediment (Supplementary Figure 6). The data were available from (Baur 2024) for the period 2018-2022. The $VAWI_{log}$ statistics across these classes were studied and a threshold value of $VAWI_{log} >= 0$ (vs. the more restrictive threshold value of $VAWI_{log} >= -0.1$ available in the original publication) was selected to identify the presence of water. In addition, sediment moisture data and punctual water depth measurements at the location of an eddy covariance station (Baur et al. 2024) were used to assess the effectiveness of $VAWI_{log}$ to track the presence of water. The extended *Flooding in Landsat Across Tidal Systems* (FLATS+) index (Julien et al. 2025) was also tested for the purpose of masking absence/presence of water and provided an additional baseline to detect open water area (FLATS+>=0.2). The results are presented in the supplementary material.

2.2.3. Climatic data

Daily water level records and monthly groundwater level data from various gauge stations were obtained from the Austrian eHYD platform (Bundesministerium für Land- und Forstwirtschaft Klima- und Umweltschutz Regionen und Wasserwirtschaft 2025). These data were used to contextualise long-term vegetation growth dynamics and assessing potential correlations with reed vitality. To align with the EVI time series, the daily water level records were averaged monthly.

Daily air temperature data at a height of two meters were obtained from a weather station in the town of Neusiedl am See (northwest shore of the lake) and were provided by GeoSphere Austria (GeoSphere Austria 2024). These values were also aggregated into monthly averages to align with the EVI data temporally. These temperature records were used to assess potential correlations between temperature conditions and long-term reed vitality through statistical analysis.

2.3. Methodological approach

The analysis of the relationship between reed vitality and water level was based on functional reed classes that were derived using an unsupervised k-means clustering of the Landsat monthly data for (1) each year separately and for (2) all years stacked together from 1985 to 2025. Each cluster was subsequently interpreted using existing reed maps. The methodology used to produce and describe the clusters is presented in §2.3.1. The results report the class mapping, the EVI climatology and its relation to elevation and position within the reed clusters.

Following the definition of functional reed classes, the focus was on the extreme drought event that occurred in 2022, which we discuss in relation to the mild 1990 and more severe 2003 water level anomalies (see §2.3.2 for details). We analysed the dynamics of reed growth in relation to EVI statistics of the 3 years precedent and after the drought year. Additionally, we conducted a sensitivity analysis of EVI in relation to seasonal variations in the surface water level and air temperature. This analysis, provided as supplementary materials, aims at understanding how water level and air temperature are driving reed vitality at the Lake Neusiedl on a seasonal basis. For this purpose, we calculated monthly means and anomalies (z-scores) for the period 1985–2025 and associated them with EVI using linear models. The slope and significance of these associations are reported for each cluster and month. We further studied the interaction between surface water level and air temperature by adding an interaction term to the linear model. Results are presented as supplementary material.

Satellite data processing (retrieval, masking, compositing and clustering) was performed using Google Earth Engine, while statistical analysis was performed in R programming.

2.3.1. Reed spatial clustering

The Landsat monthly composites from April to October (1985–2025) were concatenated into a single multiband image ordered by time, with one band per month (EVI) at 30 m resolution. Using this image stack, an unsupervised k-means (wekaKMeans, k=5) clustering was performed to group pixels with similar EVI trends. The model was initialised using 5000 randomly sampled pixels across the region of interest. The resulting cluster centroids were then used to cluster the full stack and produce a lake-wide cluster map. The number of clusters was chosen based on an elbow-method evaluation (Thorndike, 1953), where 5 represented a good balance between model simplicity and explained variance. Individual year cluster maps were also produced, allowing us to track how the spatial aggregation of vegetation clusters evolved from year to year. To assess the relevance of the unsupervised clustering, we compared the clusters to the age map developed by (Nemeth and Dvorak 2022). This map is based on aerial photographs taken annually, combined with expert knowledge of the area. Each year, zones that have been burned, harvested, or flattened in preparation for harvest are reset to age zero, while all other reed areas are incremented by one year. As such, the map reflects the time since the last disturbance, rather than the biological age or vitality of the reed. To support the ecological interpretation of the spectral clusters, we conducted a visual comparison with the latest reference classification system developed both for the Austrian and the Hungarian sides (Márkus et al. 2009; Csaplovics and Schmidt 2011). This reference dataset was created through manual segmentation of aerial imagery, combined with expert field knowledge, and distinguishes five reed classes based on structural and ecological characteristics. The comparison aimed primarily to help assign ecological meaning to the unsupervised EVI-based cluster by identifying their spatial overlap with known reed types. A comparison is provided in Supplementary Figure 1-3.

2.3.2. Influence of extreme water fluctuations

To study the influence of extreme water fluctuations on vegetation vitality during hydrological drought events, we analysed the EVI at a fixed index month (e.g. June 2022) and compare it to the same month in the antecedent two and three years (e.g. June 2019 and 2020) and the subsequent two and three years (e.g. June 2024 and 2025). The analysis was performed on three specific drought years (1990, 2003 and 2022), referred to as index years in the following, that presented negative water level anomalies in the 1985-2025 period. Notably, 2022 saw the most significant

decline in water levels. Since spring 2022, water levels had fallen below the previous negative record from autumn 2003-spring 2004, as well as the fluctuation envelope observed in records since 1965. This resulted in a new historical minimum. Although positive rainfall anomalies from spring 2023 alleviated the situation, the water level has not yet returned to long-term mean levels. For each cluster and period, we summarized EVI by its mean and computed pairwise differences between periods (e.g., index vs. −2 years, index vs. −3 years, +2 years vs. index, +3 years vs. index). Statistical significance was assessed with two-sided permutation tests that resample group labels to generate the null distribution of the mean difference. The analysis was performed using randomly stratified (by cluster) samples for a total of 1500 fixed locations. Where a cluster lacked data for a given period, that comparison was omitted for that cluster. To provide an overall conclusion across clusters, we aggregated the cluster-level differences and used a sign-flip permutation test to evaluate whether the average difference across clusters differed from zero. We visualized distributions and means by period using box plots. Multiple testing across years and clusters was addressed using two-side p-values ($\alpha = 0.01$).

To examine how changes in vegetation vigour are spatially distributed across the canopy, we binned pixels by June EVI into five quantiles (Q1–Q5, from lowest to highest EVI) for each year. We then computed interannual differences: $\Delta\mathrm{EVI}_t = \mathrm{EVI}_{\mathrm{June},t} - \mathrm{EVI}_{\mathrm{June},t-1}$ where $\Delta\mathrm{EVI}_t$ is grouped according to the June EVI quantile in year t. As an example, $\Delta\mathrm{EVI}_{2023} = \mathrm{EVI}_{\mathrm{June},2023} - \mathrm{EVI}_{\mathrm{June},2022}$ is assigned to the quantile determined by $\mathrm{EVI}_{\mathrm{June},2023}$. Similarly, we grouped $\Delta\mathrm{EVI}_t$ by elevation classes to assess how vertical position in the wetland modulates year-to-year changes.

As the June phenology might not be comparable across years, the shifts in green-up timing can affect ΔEVI and they need to be interpreted carefully. The spatial variability in changes should however not be impacted. All analyses were conducted in R (tidyverse, ggplot2, and custom permutation routines).

3. Results

3.1. Landsat time series and clustering

The Landsat EVI records (1985–2025) captured the expected seasonal cycle of reed growth, with greening in spring, peak values in early summer, and senescence during late summer and autumn. This pattern was consistent across the reed belt. The unsupervised clustering of growing-season EVI time series distinguished five functional reed classes. These ranged from clusters with high, stable EVI (dense, photosynthetically active stands in Cluster 5) to clusters with low and variable EVI (partially degraded or collapsed stands in Cluster 1) as shown in Figure 2 using the 40-year stack clustering. The spatial distribution of clusters broadly corresponded to previously published reed classifications based on aerial imagery and expert field surveys (e.g., Csaplovics & Schmidt, 2011; Márkus et al., 2009), providing confidence in the unsupervised clustering of the different ecological functional groups as described in Table 1. The clustering performed on single years further consolidated the results observed with the clustering of the 40-year stack with similar temporal and spatial patterns (Fig. D) and it additionally allowed to study how year-to-year transitions of pixels between clusters occur as shown in Appendix (Fig. E) along with the climatological EVI values for each cluster.

Table 1 Cluster number and description ecological functional groups. The mean elevation in meters above sea level (m a.s.l., Adriatic datum) of the clusters is also provided. For reference (using the period 1965-2025 as baseline), the mean water level is 115.50 m a.s.l. with water levels that ranges from a high of 115.58 m a.s.l. (SD = 0.17) in April to a low of 115.39 m a.s.l. (SD = 0.17) in September. The historical low is 114.88 m a.s.l. touched in October 2022, preceded only by the low of 115.07 m a.s.l. reached in October 2003.

Cluster number	Associated Class in Csaplovics et al. (2009)	Typical July EVI Range (p25–p75)	Description	Mean elevation m a.s.l.

5	Class I	0.60–0.63	Very vigorous reed	115.75
4	Class II + class III.Aa in the Wulka delta only	0.45–0.54	Vigorous reed High biomass, tall reed, consistent seasonal productivity.	115.73
3	class III.A	0.39–0.49	Healthy but aging / mixed reed Slight senescence or patchiness, possible heterogeneity, still functionally strong.	115.69
2	class IV.A	0.30–0.35	Structurally degraded reed Gaps, fragmentation, potential invasion by Typha or other species.	115.64
1	Class V + brown water	0.20–0.24	Non-productive / collapsed system Dead reed, mudflat, brown water areas, post-disturbance, open water encroachment.	115.62

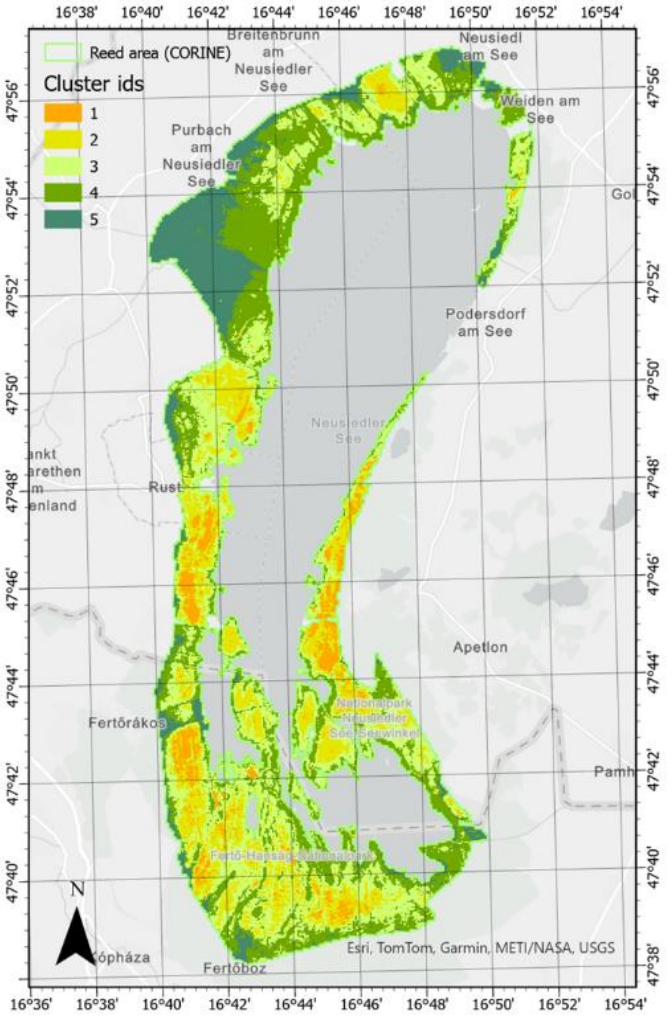

Figure 2 Results of the pixel clustering of the reed area around the Lake Neusiedl using the 40-year stack of data. The clusters were used to spatially aggregate EVI values and to analyse the functional relationships with water levels.

3.2. Influence of interannual water fluctuations during extreme drought events

We analysed the EVI in June for the three drought events (referred to the index years: 1990, 2003 and 2022) and compared it with the same month in the antecedent and subsequent years. Figure 3 and Figure 4 shows the standardized monthly anomalies for air temperature, rainfall and water levels providing a picture of the climatic fluctuations in the period of analysis.

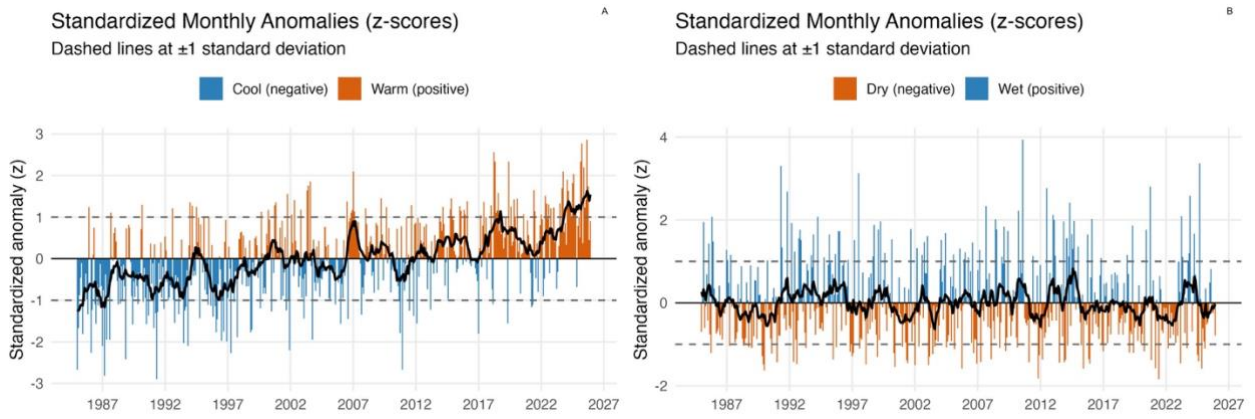

Figure 3 Air Temperature (panel A, left) and Rainfall (panel B, right) anomalies (z-score calculated on the baseline 1985-2025).

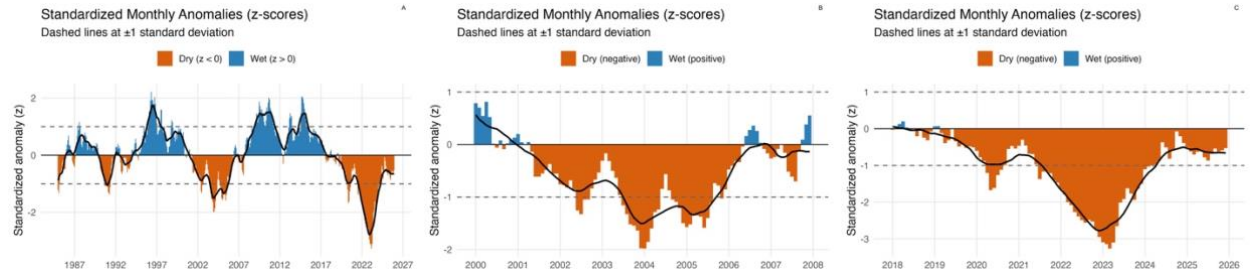

Figure 4 Surface Water Level anomalies (standardized monthly anomalies with ±1σ bands calculated on the baseline 1985-2025) for the study region (panel A) and details of the 2003 (panel B) and 2022 (panel C) drought events.

The index years were selected based on records of the lowest water levels (Figure 4) and corresponded to years in which the SWL (monthly mean) reached approximately 30 cm, 40 cm and 60 cm below the mean water level. EVI in June was extracted in 2000 random stratified point locations, masked ($VAWI_{log}$ >= 0) and grouped by cluster and year for the analysis. Based on these observations, we present cluster-level contrasts (e.g. index year vs +3y) and a pooled across-cluster estimate, with uncertainty assessed via two-sided permutation tests. No statistically significant trends were found for 1990 or 2003; in contrast, 2022 exhibits a clear and statistically significant trend. In 2022, the EVI distributions are similar across clusters, and they display a noticeable upward shift at +2y (2024) and +3y (2025) (see Figure 5).

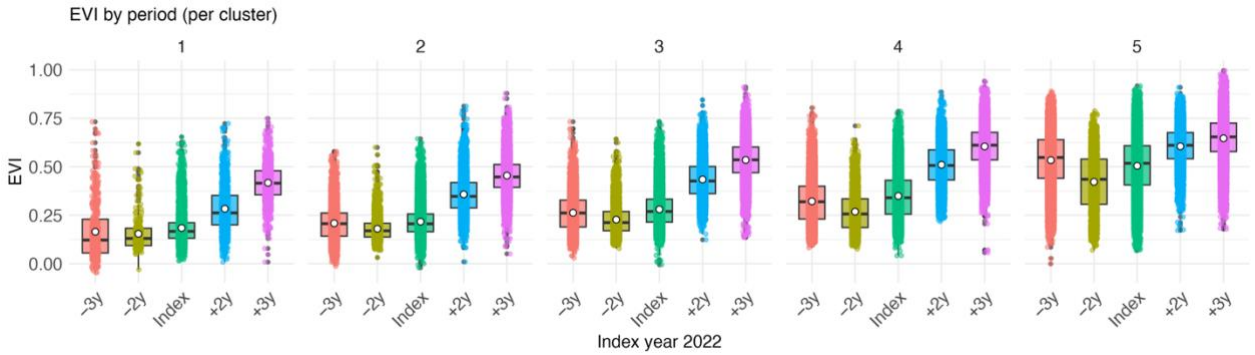

Figure 5 EVI per-cluster and period in relation to the 2022 index year (y).

Across the 5 clusters, the mean difference between the index year (June 2022) and the +2y (June 2024) and +3y periods (June 2025) was positive (permutation test, two-sided $p < 0.01$). For example, EVI in 2025 exceeded 2022 by 0.26 ($p < 0.01$) for C2, by 0.24 ($p < 0.01$) for C3 and by 0.25 ($p < 0.01$) for C4. A more moderate increase of 0.14 was observed for C5. Pooled (across C1-C5) differences of +0.13 (at +2y) and +0.22 (at +3y) in EVI correspond to a moderate increase in vegetation greenness. Figure 6 maps the spatial distribution of the difference between year pairs showing mostly stable or moderate decline in growth at +1y, a general strong growth at + 2y and moderate to stable condition at +3y. Figure 7 summaries how changes are distributed: at +1y, conditions are broadly stable. pixels in the lowest EVI quantile (Q1) tend to decline slightly, whereas the highest quantile (Q5) shows modest gains. The largest and most significant increases occur at +2y, with positive ΔEVI across all quantiles. By +3y, changes are again small overall, with denser reed stands (higher quantiles) benefiting the most. Figure 8 provides the corresponding June EVI maps for visual reference. Grouping by elevation (Figure 9) indicates that at +1y, most gains occur at higher elevations. At +2y, growth shifts to lower elevations and remains evident at +3y, albeit with reduced magnitude. Although reed growth has reached the climax in June, absolute differences between years need to be interpreted carefully as phenology might not be aligned across the years.

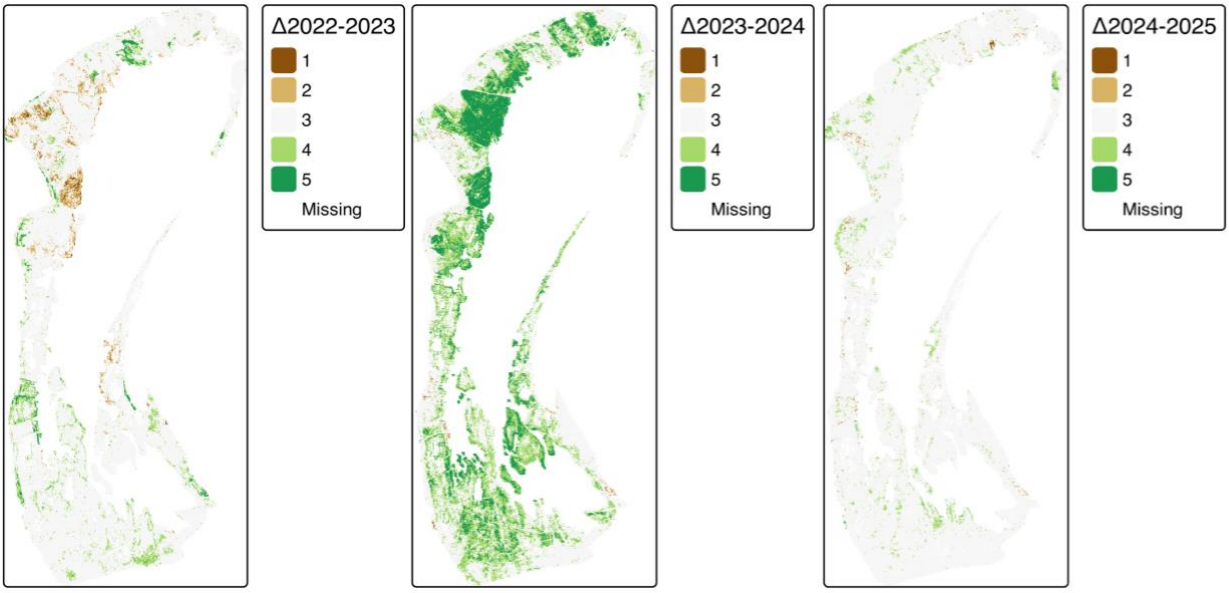

Figure 6 Differences in EVI (ΔEVI) calculated at +1y (2023), +2y (2024) and +3y (2025) after the extreme low water year 2022. Categories 1: Strong decline: $\Delta \leq -0.25$; 2: Moderate decline: $-0.25 < \Delta \leq -0.15$; 3: Stable: $-0.15 < \Delta < 0.15$; 4: Moderate growth: $0.15 \leq \Delta < 0.25$ and 5: Strong growth: $\Delta \geq 0.25$.

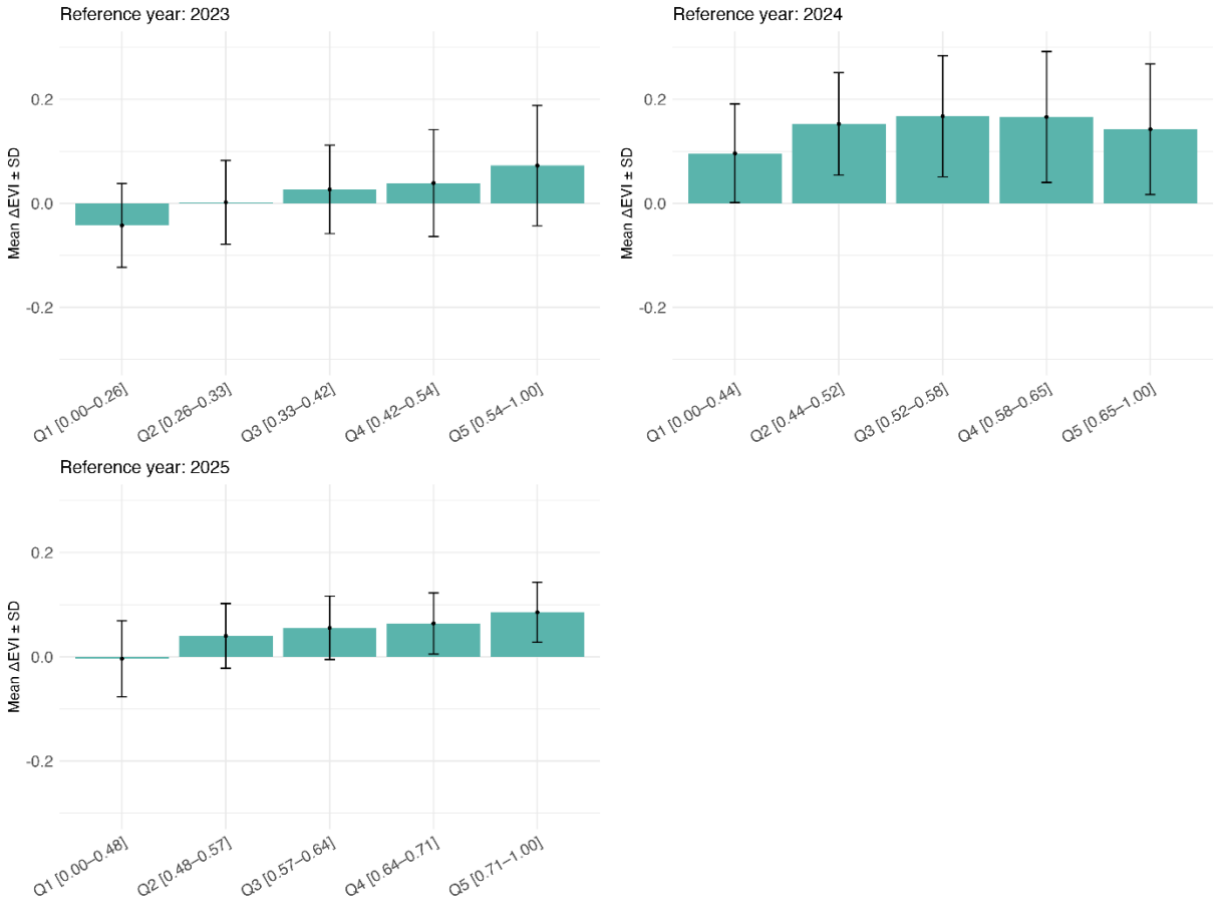

Figure 7 Distribution of the ΔEVI by EVI values (using quantile bins) at +1y, +2y and +3y.

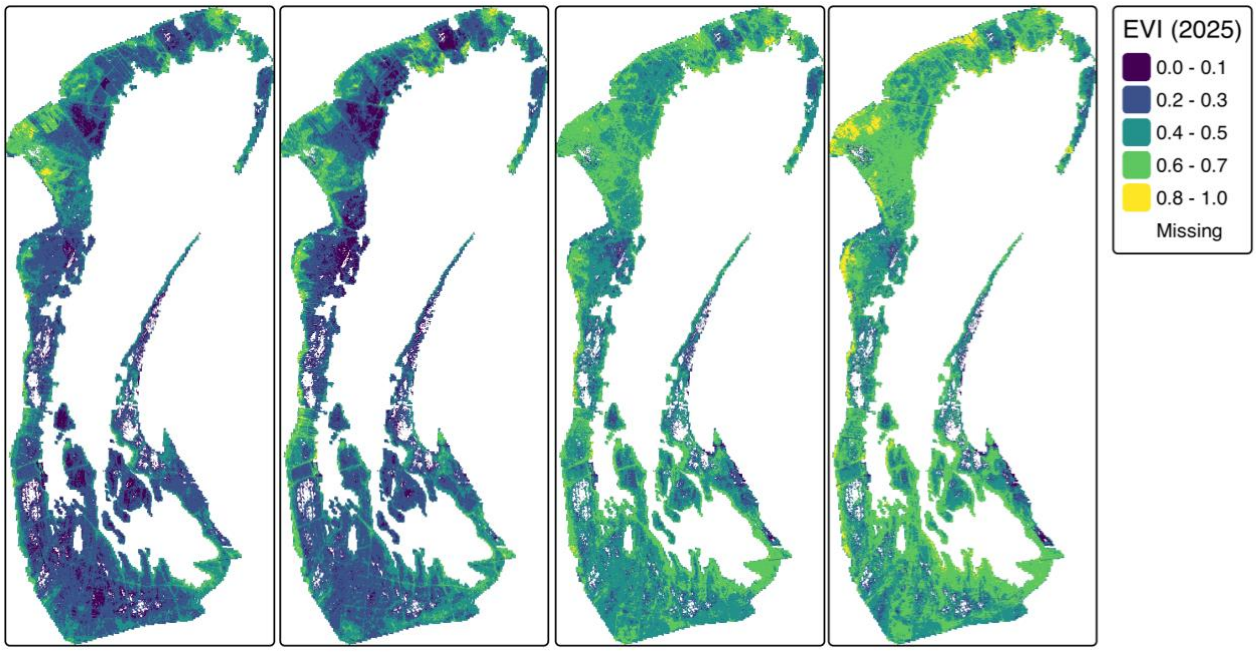

Figure 8 Mean EVI in June for the years 2022 (index), 2023 (+1y), 2024 (+2y) and 2025 (+3y)

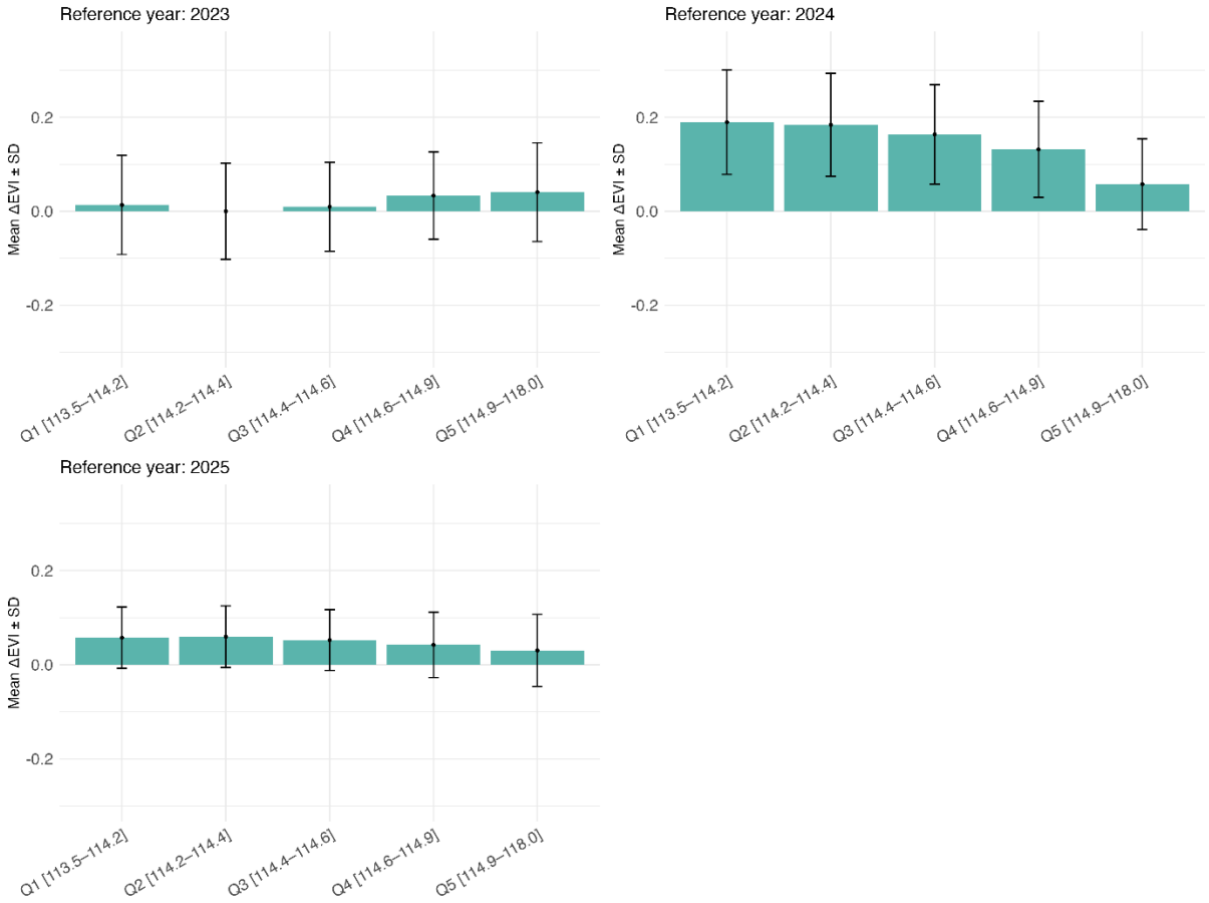

Figure 9 Distribution of the ΔEVI by elevation (using quantile bins) at +1y, +2y and +3y.

For the 1990 index year (see Figure 10), differences were small ($|\Delta| < 0.09$, $p > 0.12$), and for 2003 (see Figure 11) they were also small ($|\Delta| < 0.04$, $p > 0.30$), with generally negative shifts at +2y and +3y. These results are consistent with the comparatively mild hydrological droughts in 1990 and 2003.

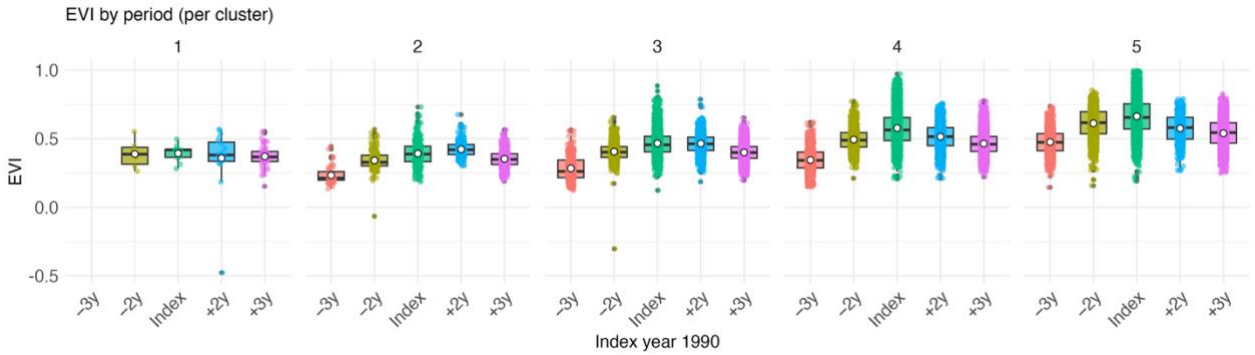

Figure 10 EVI per-cluster and period in relation to the 1990 index year (y).

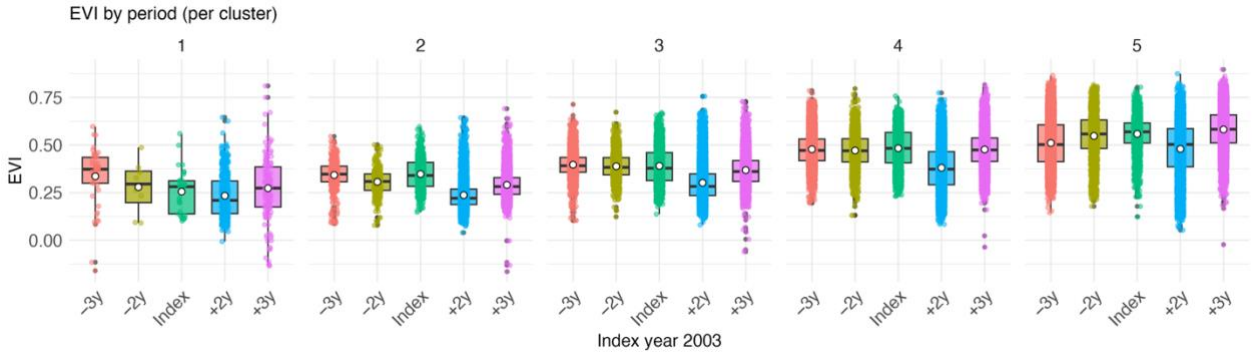

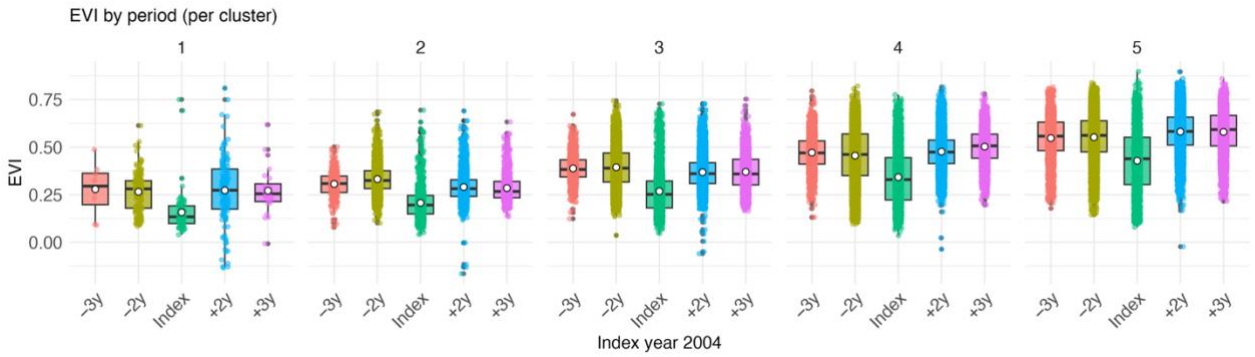

Figure 11 EVI per-cluster and period in relation to the 2003 and 2004 index year (y). For 2003, we illustrate both the 2003 and 2004 considered as "index year" as the drought might have impacted mostly 2004.

4. Discussion

The analysis of the three extreme water fluctuation events provides the most consequential finding of our study which relates not to the decline of the reed stands itself, but rather the subsequent recovery and the underlying conditions that led to it. The variability of the habitat and the connected status of *Phragmites australis* in Lake Neusiedl is obvious to observers, as the morphological and physiological differences of the plants in-situ are apparent and have seemingly remained constant until now (Tóth 2025). The trajectories of EVI from 2018 to 2022 closely mirror the fine-scale trends reported by (Baur et al. 2024) near Illmitz. Baur et al. (2024) notes that this period sees a gradual increase in EVI from 2018 to 2021, with a sharp collapse in 2022, when the intensity of the drought peaked and the lake reached historically low water levels. These dynamics are also confirmed by our dataset. However, our analysis covers an additional three years after the drought and shows a robust rebound in 2024 and 2025 that exceeded all highs seen during earlier years of drought. By extending this evidence to a full-lake, four-decade perspective, our results reveal how the resilience and rebound capacity of *Phragmites australis* after 2022 is different. Our data do not evidence a similar rebound of vegetation after the 1990 and 2003 drought period.

The physiologically robust and spatially extensive rebound in reed vitality following the historically unprecedented drawdown at Lake Neusiedl in 2022 compels us to fundamentally re-examine the prevailing management logic governing shallow (not only steppe) lakes. The assumption in wetland conservation that water retention and hydrological stability are inherently protective may represent an ecological fallacy with measurable consequences for the status and presence of reeds in the specific context of Phragmites-dominated shallow lakes.

Water movements impact numerous ecological and limnological functions, affecting not only aquatic plants but broader aquatic ecosystems (SandJensen and Pedersen 1999; Madsen et al. 2001; Lacoul and Freedman 2006). Water level and fluctuations significantly impact macrophyte growth (Asaeda et al. 2009; Bornette and Puijalon 2011; Krolová et al. 2013; Tóth 2016). Water depth can constrain plant growth by limiting oxygen availability (Armstrong et al. 2000; Cizková et al. 2001; Tóth 2016). Emergent macrophytes adjust to static water depths (Vretare et al., 2001; Krolová et al., 2013; Tóth, 2016) through similar acclimations observed in this study. *Phragmites australis* does not evolve in stable hydrological environments. Shallow endorheic lakes, such as those in the Pannonian Basin, are geologically and climatically predisposed to extreme variability, including complete desiccation events (Korponai et al. 2010; Jeppesen et al. 2014; Borics et al. 2016). For example, Lake Neusiedl experienced such an event between 1865 and 1870. The ecological succession trajectory of such systems typically progresses from an open, shallow lake to an emergent macrophyte belt dominated initially by *Phragmites*, and then to increasingly terrestrial communities, including wet meadows, fens, and eventually mesic grasslands or woodlands,

depending on the regional climate (Carpenter 1981). This successional pathway is not linear, but is punctuated and reset by disturbance events, particularly hydrological extremes, which prevent any single successional stage from reaching competitive closure (Odland and Del Moral 2002). In this evolutionary context, the 2022 drought was not an anomalous catastrophe, but rather a large-magnitude instance of the disturbance regime through which the reed belt developed.

The reed vigorous response, with pooled EVI gains of +0.13 two years post-drought and +0.22 three years post-drought, is consistent with a plant community that retains the physiological and demographic capacity to exploit post-disturbance resource pulses, provided the disturbance is of sufficient magnitude. The implications for management are clear, although they may present certain challenges. Since 1965, the regulation by the weir of the Einser-kanal (Hanság-főcsatorna) has been made to maintain a water level as constant as possible and to prevent both floodings and low water levels. However, this may have inadvertently suppressed the oxidation events that the reed belt requires for periodic renewal. By maintaining stable water levels relative to those that would have been produced by unmanaged, climatically driven dynamics, this defensive strategy has likely prolonged anoxic conditions in the rhizosphere and deepened the litter accumulation bottleneck that underlies chronic reed die-back. In this system, stability is not neutral; it is a slow-acting stressor. The sensitivity analysis to water level and air temperature on a seasonal basis further show (in Supplementary material) that the associations are weak or neutral.

A comparative analysis of the three drought index years (1990, 2003 and 2022) shows that hydrological stress does not linearly translate into ecological benefit. No statistically significant productivity rebound was detected following the 1990 or 2003 events. In fact, the 1990 period was even associated with weakly negative EVI shifts two and three years after the drought. A limnologically compelling explanation is that the 1990 and 2003 droughts were not severe or long-lasting enough to aerate the deeper zones of sediment containing organic matter that had accumulated over decades due to reduced decomposition under permanently or nearly permanently inundated conditions. While the 2003 event reached a minimum of approximately 115.07 m a.s.l. in October of that year, the 2022 event descended to 114.88 m a.s.l. (roughly 19 cm lower), representing not merely an extension of drought severity, but a qualitatively different exposure of the sediment surface given the extreme shallowness of this lake. With a mean lake depth of around 120 cm and a maximum depth of 180 cm, a 19 cm difference in minimum water level (a ~16% decrease in water depth) corresponds to a significant increase in the proportion of lakebed and reed rhizosphere exposed to atmospheric oxygen. The 1990 event reached only approximately 30 cm below the long-term mean and therefore almost certainly failed to expose the deep anoxic organic horizons. Therefore, in this system, reed vitality does not operate as a continuous function of water availability; it is not in a linear relationship with the level of inundation. Rather, it operates as a pulse-response system, in which ecological rejuvenation requires crossing a critical threshold of exposure depth and duration. This threshold must be sufficient to penetrate and oxidise the accumulated litter and sediment organic matter that constitute the primary driver of long-term die-back.

The mechanism underlying the post-2022 rebound is almost certainly rooted in sediment biogeochemistry rather than canopy-level water relations. Wide-scale detailed field measurements do not exist and we can only assume that during the 2022 drawdown, the transition from anaerobic to aerobic conditions across large areas of the lakebed dramatically accelerated the microbial mineralisation of accumulated organic matter, such as organic nitrogen, phosphorus and carbon, which had been locked in slowly decomposing litter under reducing conditions for potentially decades. This shift in redox chemistry effectively fertilised the area, releasing nutrients into the rooting zone at a time when improved drying conditions also increased oxygen availability for root respiration. The result is a reduced accumulation of phytotoxic compounds, restored aerobic

metabolic capacity in rhizomes and a nutrient pulse that supports rapid shoot production in subsequent growing seasons. This mechanism is analogous to the changes registered in Lake Balaton (Tóth 2016), in which redox potential measurements in rhizosphere sediments were significantly higher following the 2003 drought. Similar observations were made in other lakes of the world (Golosov et al. 2012; Couture et al. 2015). This oxygenation occurred at the same time as the restoration of vigour in senescent *Phragmites* stands. The EVI increase of +0.26 in Cluster 2 by 2025 is particularly revealing because it indicates that the nutrient release was sufficient to stimulate recovery, even in stands where chronic stress had severely compromised biomass and canopy structure. We strongly assume that this is not the response of a system merely relieved of inundation stress; it is the response of a system that has received a substantial biogeochemical subsidy from the oxidation of its accumulated organic matter.

The spatial sequence of recovery adds a further mechanistic layer that reinforces the oxygen-priming interpretation. Areas at higher elevations within the reed belt showed the earliest gains, with modest positive EVI anomalies already apparent one year after the drought. In contrast, lower-elevation zones, which experienced shorter or less complete exposure during the drawdown, showed their largest gains two years after the drought, with residual but diminishing benefits three years after the drought. This lag could not be adequately explained by differences in water depth alone. Higher ground dries out more quickly and remains dry for longer. This results in a longer period of sediment oxidation and aerobic microbial activity before subsequent inundation. By the time the spring water levels returned in 2023, the rhizosphere at higher elevations had already undergone the necessary redox transition to support vigorous regrowth. However, root zones at lower elevations were still recovering from prolonged anoxia. These zones required additional time for aerobic microbial communities to establish and complete mineralisation, resulting in a delay of a full growing season. This oxygen-priming sequence, in which the duration of sediment aeration rather than its mere occurrence determines the timing and magnitude of the canopy's response, has direct implications for managed drawdown strategies.

Overall, the results provide quantitative evidence at the lake scale for a long-debated ecological mechanism: *Phragmites australis*, in large shallow systems such as Lake Neusiedl, thrives under moderate hydrological fluctuation but declines under persistent flooding or prolonged dry periods.

The robust recovery observed after the 2022 low-water level attests that variability, rather than hydrological stability, may be required to guarantee reed stability over the long term. From a management perspective, fluctuations correspond with recommendations for mitigating reed die-back through the deliberate use of water-level variability (Krolová et al., 2013).

4.1. Management Implications

Lake Neusiedl is strongly embedded in human activities. Its proximity to major Central European cities such as Vienna, Bratislava, and Győr makes it a key site for tourism and various economic activities rely on it. Being the largest lake in Austria, Neusiedl plays an important role in regional recreation and water sports. In 2024, the region recorded over 1.7 million overnight stays, accounting for more than half of all overnight stays in Burgenland (Statistik Burgenland 2024). Yet, in recent years persistently low water levels have raised concerns about the sustainability of the recreational and nautical activities. In response to ongoing drought, local authorities are considering an artificial water supply from the Danube, a decision that remains highly debated (Der Standard 2024). The complexity of these debates reflects the need for a multi-level understanding of issues affecting Lake Neusiedl, integrating aspects such as reed dynamics, water availability, tourism, and climate change. Research has long focused on the lake’s hydrology and water balance, which is strongly dependent on atmospheric factors, with direct precipitation contributing around 79% of water input (Soja et al. 2013). The lake has historically shown vulnerability to fluctuations in water level, with a complete drying event between 1865 and 1870, while the construction of the

Einser-kanal in 1909 and later hydraulic controls in 1965 altered the natural regime (Tolotti et al. 2021). Limnological studies have further reconstructed its hydrological and ecological evolution in the last 160 years, demonstrating a long-term sensitivity to climate (Tolotti et al. 2021).
The results of our study lead to some practical considerations for managing the reed belt of Lake Neusiedl. Vitality differs strongly between outer, dynamic zones and managed stands, which tend to remain stable or improve, and interior, stagnant areas, where decline is more persistent. This suggests that management should be adapted to local conditions rather than applied in the same way everywhere. In all cases, however, reducing accumulated biomass is necessary to reduce die-back and support reed vitality (Hazelton et al. 2014; Nemeth and Dvorak 2022). This can be achieved through hydrological variation, targeted harvesting, or, in certain contexts, burning.

Future climate projections (Soja et al. 2013; Tolotti et al. 2021) indicate more frequent water deficits and a recent study predicts a higher probability of droughts but also wetter overall conditions (Haslinger et al. 2023). As already slightly indicated in Figure 4, water anomalies may become more frequent. Consequently, long periods of low water can shift reed distribution, and fluctuations may help to rejuvenate older stands by improving sediment oxygenation and so reducing accumulated biomass. Currently, an artificial water supply from the neighbouring river Danube is planned mainly to guarantee higher water levels for recreational boating and water sports. The considered threshold for a water supply is 115.2 m. a.s.l. (Wolfram et al. 2020). With this regulation the last low water level of 2022 (minimum of 114.88 m. a.s.l.) would never have been reached, and the reed would not have been able to regenerate under such conditions. If large-scale measures such as diverting Danube water into the lake are considered, they should thus be designed in a way that supports reed vitality, by avoiding prolonged flooding in sensitive areas, and still allowing some degree of natural fluctuation.
Disturbance management can also support reed vitality. Harvested zones were often in the highest vitality clusters, suggesting that more harvesting could be beneficial. Rotational harvesting, as tried in (Antoniazza et al. 2018) has already been suggested (Nemeth and Dvorak 2022), but the best timing, frequency, and access need to be defined, including the use of machinery in winters with little ice. Fire is more context dependent. In degraded, litter-filled stands burned before the growing season, productivity and structure improved, showing that fire can act as a low-intervention reset in the right conditions. In vigorous stands or after summer burns, effects were weaker or more variable. If used for conservation, fire should be carefully timed and matched to site condition and water regime.
The strong spatial contrasts in reed vitality mean that location-specific strategies are needed. Lakeward reeds may require little active intervention, while interior zones with ongoing decline are more likely to benefit from disturbance or improved hydrological connections. Detailed elevation and hydrological mapping could help to identify vulnerable areas and guide interventions.

5. Conclusion

This research used forty years of satellite data to describe the growth dynamics of the reed belt at Lake Neusiedl. It is one of the first studies spanning forty years and covering the entire lake, making it possible to quantify the interactions between hydrology, climate and reed vigour in terms of time and space. By combining EVI data with hydrological and climatic records, it demonstrated how reed vigour responds weakly to short-term seasonal variations and particularly to extreme changes in water level. From a spatial perspective, the analysis highlighted significant contrasts between managed or well-oxygenated areas and stagnant areas further inland. Beyond Lake Neusiedl, this study demonstrates the value of using long-term time series to analyse the resilience of reed in shallow lake context. This approach provides a reusable framework for tracking the historical evolution of reed beds. Continuously integrating satellite time series with in-situ observations will be essential for anticipating future changes of the reed in a changing climate.

6. Author Contributions Statement

Francesco Vuolo: Conceptualization, Methodology, Formal analysis, Supervision, Writing – original draft
Matthieu Collet: Conceptualization, Formal analysis, Writing – original draft
Rasmus Fensholt: Supervision, Methodology
Erwin Nemeth: Conceptualization, Methodology, Writing – original draft, Writing – review & editing
Viktor Toth: Conceptualization, Methodology**,** Writing – original draft, Writing – review & editing

7. Bibliography

Antoniazza, M., Clerc, C., Le Nédic, C., Sattler, T., & Lavanchy, G. (2018). Long-term effects of rotational wetland mowing on breeding birds: evidence from a 30-year experiment. *Biodiversity and Conservation*, *27*(3), 749–763. https://doi.org/10.1007/s10531-017-1462-1

Armstrong, W., Cousins, D., Armstrong, J., Turner, D. W., & Beckett, P. M. (2000). Oxygen distribution in wetland plant roots and permeability barriers to gas-exchange with the rhizosphere: a microelectrode and modelling study with Phragmites australis. *Annals of Botany*, *86*(3), 687.

Asaeda, T., Siong, K., Kawashima, T., & Sakamoto, K. (2009). Growth of Phragmites japonica on a sandbar of regulated river: morphological adaptation of the plant to low water and nutrient availability in the substrate. *River Research and Applications*, *25*(7), 874–891.

Baibagyssov, A., Magiera, A., Thevs, N., & Waldhardt, R. (2025). Resource Characteristics of Common Reed (Phragmites australis) in the Syr Darya Delta, Kazakhstan, by Means of Remote Sensing and Random Forest. *Plants*, *14*(6), 933. https://doi.org/10.3390/plants14060933

Ballut-Dajud, G. A., Sandoval Herazo, L. C., Fernández-Lambert, G., Marín-Muñiz, J. L., López Méndez, M. C., & Betanzo-Torres, E. A. (2022). Factors Affecting Wetland Loss: A Review. *Land*, *11*(3), 434. https://doi.org/10.3390/land11030434

Baur, P. A. (2024). *Multi-year data set of vegetation indices of the wetland with reeds at Lake Neusiedl from 2018 to 2022*. V1. PHAIDRA Repositorium (University of Vienna).

Baur, P. A., Maier, A., Buchsteiner, C., Zechmeister, T., & Glatzel, S. (2024). *Consequences of intense drought on CO 2 and CH 4 fluxes of the reed ecosystem at Lake Neusiedl*. https://doi.org/10.25365/phaidra

Bedford, A. P. (2005). DECOMPOSITION OF PHRAGMITES AUSTRALIS LITTER IN SEASONALLY FLOODED AND EXPOSED AREAS OF A MANAGED REEDBED. In *WETLANDS* (Vol. 25, Number 3).

Bertassello, L. E., Basu, N. B., Maes, J., Grizzetti, B., La Notte, A., & Feyen, L. (2025). The important role of wetland conservation and restoration in nitrogen removal across European river basins. *Nature Water*, *3*(8), 867–880. https://doi.org/10.1038/s44221-025-00465-0

Borics, G., Ács, É., Boda, P., Boros, E., Erős, T., Grigorszky, I., Kiss, K. T., Lengyel, S., Somogyi, B., & Vörös, L. (2016). Water bodies in Hungary–an overview of their management and present state. *Hidrológiai Közlöny*, *96*(3), 57–67.

Bornette, G., & Puijalon, S. (2011). Response of aquatic plants to abiotic factors: a review. *Aquatic Sciences-Research Across Boundaries*, (73), 1–14.

Buchsteiner, C., Baur, P. A., & Glatzel, S. (2023). Spatial Analysis of Intra-Annual Reed Ecosystem Dynamics at Lake Neusiedl Using RGB Drone Imagery and Deep Learning. *Remote Sensing*, *15*(16), 3961. https://doi.org/10.3390/rs15163961

Bundesministerium für Land- und Forstwirtschaft Klima- und Umweltschutz Regionen und Wasserwirtschaft. (2025). *eHYD – der Zugang zu hydrographischen Daten \" {Osterreichs*. https://ehyd.gv.at/

Carpenter, S. R. (1981). Submersed vegetation: an internal factor in lake ecosystem succession. *The American Naturalist*, *118*(3), 372–383.

Cizková, H., Istvánovics, V., Bauer, V., & Balázs, L. (2001). Low levels of reserve carbohydrates in reed (Phragmites australis) stands of Kis-Balaton, Hungary. *Aquatic Botany*, *69*(2–4), 209–216. https://doi.org/doi: DOI: 10.1016/S0304-3770(01)00139-5

Čížková, H., Kučera, T., Poulin, B., & Květ, J. (2023). Ecological Basis of Ecosystem Services and Management of Wetlands Dominated by Common Reed (Phragmites australis): European Perspective. *Diversity*, *15*(5), 629. https://doi.org/10.3390/d15050629

Couture, R., de Wit, H. A., Tominaga, K., Kiuru, P., & Markelov, I. (2015). Oxygen dynamics in a boreal lake responds to longterm changes in climate, ice phenology, and DOC inputs. *Journal of Geophysical Research: Biogeosciences*, *120*(11), 2441–2456.

Csaplovics, E. (1982). *Interpretation von Farbinfrarotbildern : Kartierung von Vegetationsschäden in Brixlegg ; Schilfkartierung Neusiedler See* (Vol. 23). Techn. Univ., Wien. https://repositum.tuwien.at/handle/20.500.12708/533

Csaplovics, E. (2019). Der Schilfgürtel des Neusiedler Sees. *Österreichische Wasser- Und Abfallwirtschaft*, *71*, 494–507. https://doi.org/10.1007/s00506-019-00622-2

Csaplovics, E., & Schmidt, J. (2011). Schilfkartierung Neusiedler See, Ausdehnung und Struktur der Schilfbestände des Neusiedler Sees-Projektmanagement, Erfassung und Kartierung des österreichischen Anteils durch Luftbildklassifikation. *Projekt-Abschlussbericht, OeNB Burgenland, Eisenstadt, Dresden*.

Declaro, A., Brown, Z., & Kanae, S. (2025). VAWIlog: A Log-Transformed LSWI–EVI Index for Improved Surface Water Mapping in Agricultural Environments. *Remote Sensing*, *17*(16), 2771. https://doi.org/10.3390/rs17162771

Der Standard. (2024). *Die Donau könnte bald ins Burgenland flie\ss{}en*. https://www.derstandard.at/story/3000000234858/die-donau-koennte-bald-ins-burgenland-fliessen

European Environment Agency. (2019). *CORINE Land Cover 2018 (vector), Europe, 6-yearly - version 202020u1*. https://doi.org/10.2909/71c95a07-e296-44fc-b22b-415f42acfdf0

Fluet-Chouinard, E., Stocker, B. D., Zhang, Z., Malhotra, A., Melton, J. R., Poulter, B., Kaplan, J. O., Goldewijk, K. K., Siebert, S., Minayeva, T., Hugelius, G., Joosten, H., Barthelmes, A., Prigent, C., Aires, F., Hoyt, A. M., Davidson, N., Finlayson, C. M., Lehner, B., … McIntyre, P. B. (2023). Extensive global wetland loss over the past three centuries. *Nature*, *614*(7947), 281–286. https://doi.org/10.1038/s41586-022-05572-6

Gaberščik, A., Grašič, M., Abram, D., & Zelnik, I. (2020). Water level fluctuations and air temperatures affect common reed habitus and productivity in an intermittent wetland ecosystem. *Water (Switzerland)*, *12*(10). https://doi.org/10.3390/w12102806

GeoSphere Austria. (2024). *Messstationen Tagesdaten v2*. GeoSphere Austria. https://doi.org/10.60669/GS6W-JD70

Golosov, S., Terzhevik, A., Zverev, I., Kirillin, G., & Engelhardt, C. (2012). Climate change impact on thermal and oxygen regime of shallow lakes. *Tellus A: Dynamic Meteorology and Oceanography*, *64*(1), 17264.

Graveland, J. (1998). Reed die-back, water level management and the decline of the Great Reed Warbler Acrocephalus arundinaceus in The Netherlands. *Ardea-Wageningen*, (86), 187–201.

Haslinger, K., Schöner, W., Abermann, J., Laaha, G., Andre, K., Olefs, M., & Koch, R. (2023). Apparent contradiction in the projected climatic water balance for Austria: wetter conditions on average versus higher probability of meteorological droughts. *Natural Hazards and Earth System Sciences*, *23*(8), 2749–2768. https://doi.org/10.5194/nhess-23-2749-2023

Hazelton, E. L. G., Mozdzer, T. J., Burdick, D. M., Kettenring, K. M., & Whigham, D. F. (2014). Phragmites australis management in the United States: 40 years of methods and outcomes. *AoB PLANTS*, *6*, plu001. https://doi.org/10.1093/aobpla/plu001

Herzig, A. (2014). Der Neusiedler See–Limnologie eines Steppensees. *Denisia*, *33*, 101–144.

Huete, A. R., Liu, H. Q., Batchily, K., & van Leeuwen, W. (1997). A comparison of vegetation indices over a global set of TM images for EOS-MODIS. *Remote Sensing of Environment*, *59*(3), 440–451. https://doi.org/10.1016/S0034-4257(96)00112-5

Jeppesen, E., Meerhoff, M., Davidson, T., Trolle, D., Sondergaard, M., Lauridsen, T., Beklioğlu, M., Brucet, S., Volta, P., & González-Bergonzoni, I. (2014). Climate change impacts on lakes: an integrated ecological perspective based on a multi-faceted approach, with special focus on shallow lakes. *Journal of Limnology*, *73*.

Julien, A. R., Narron, C. R., & Mishra, D. R. (2025). Expanding the flooding in Landsat across tidal systems model to Landsat 5–9 imagery for long-term marsh inundation analysis. *Science of The Total Environment*, *965*, 178602. https://doi.org/10.1016/j.scitotenv.2025.178602

Karstens, S., Inácio, M., & Schernewski, G. (2019). Expert-Based Evaluation of Ecosystem Service Provision in Coastal Reed Wetlands Under Different Management Regimes. *Frontiers in Environmental Science*, *7*. https://doi.org/10.3389/fenvs.2019.00063

Kingsford, R. T., Basset, A., & Jackson, L. (2016). Wetlands: conservation's poor cousins. *Aquatic Conservation: Marine and Freshwater Ecosystems*, *26*(5), 892–916. https://doi.org/10.1002/aqc.2709

Korponai, J., Braun, M., Buczkó, K., Gyulai, I., Forró, L., Nédli, J., & Papp, I. (2010). Transition from shallow lake to a wetland: a multi-proxy case study in Zalavári Pond, Lake Balaton, Hungary. *Hydrobiologia*, *641*(1), 225–244.

Krolová, M., Čížková, H., Hejzlar, J., & Poláková, S. (2013). Response of littoral macrophytes to water level fluctuations in a storage reservoir. *Knowledge and Management of Aquatic Ecosystems*, (408), 7.

Lacoul, P., & Freedman, B. (2006). Environmental influences on aquatic plants in freshwater ecosystems. *Environmental Reviews*, *14*(2), 89–136.

Madsen, J. D., Chambers, P. A., James, W. F., Koch, E. W., & Westlake, D. F. (2001). The interaction between water movement, sediment dynamics and submersed macrophytes. *Hydrobiologia*, *444*(1–3), 71–84.

Márkus, I., Király, G., & Börcsök, Z. (2009). Qualifikation und Klassifikation des Schilfgürtels des Neusiedler Sees (ungarischer Anteil). *WHU, Sopron*.

Nemeth, E., & Dvorak, M. (2022). Reed die-back and conservation of small reed birds at Lake Neusiedl, Austria. *Journal of Ornithology*, *163*(3), 683–693. https://doi.org/10.1007/s10336-022-01961-w

Odland, A., & Del Moral, R. (2002). Thirteen years of wetland vegetation succession following a permanent drawdown, Myrkdalen Lake, Norway. *Plant Ecology*, *162*(2), 185–198.

Ojdanič, N., Holcar, M., Golob, A., & Gaberščik, A. (2023). Environmental extremes affect productivity and habitus of common reed in intermittent wetland. *Ecological Engineering*, *189*, 106911. https://doi.org/10.1016/j.ecoleng.2023.106911

Qiu, J., Yang, J., Wang, Y., & Su, H. (2018). A comparison of NDVI and EVI in the DisTrad model for thermal sub-pixel mapping in densely vegetated areas: a case study in Southern China. *International Journal of Remote Sensing*, *39*(8), 2105–2118. https://doi.org/10.1080/01431161.2017.1420929

Rupasinghe, P. A., & Chow-Fraser, P. (2021). Mapping Phragmites cover using WorldView 2/3 and Sentinel 2 images at Lake Erie Wetlands, Canada. *Biological Invasions*, *23*(4), 1231–1247. https://doi.org/10.1007/s10530-020-02432-0

Sailer, C. L., & Maracek, K. (2019). Der Neusiedler See – ein \" {Uberblick. *Österreichische Wasser- Und Abfallwirtschaft*, *71*(11), 483–493. https://doi.org/10.1007/s00506-019-00621-3

SandJensen, K., & Pedersen, O. (1999). Velocity gradients and turbulence around macrophyte stands in streams. *Freshwater Biology*, *42*(2), 315–328.

Serrano-Ortiz, P., Aranda-Barranco, S., López-Ballesteros, A., Lopez-Canfin, C., Sánchez-Cañete, E. p., Meijide, A., & Kowalski, A. s. (2020). Transition Period Between Vegetation Growth and Senescence Controlling Interannual Variability of C Fluxes in a Mediterranean Reed Wetland. *Journal of Geophysical Research: Biogeosciences*, *125*(1), e2019JG005169. https://doi.org/10.1029/2019JG005169

Soja, G., Züger, J., Knoflacher, M., Kinner, P., & Soja, A.-M. (2013). Climate impacts on water balance of a shallow steppe lake in Eastern Austria (Lake Neusiedl). *Journal of Hydrology*, *480*, 115–124. https://doi.org/10.1016/j.jhydrol.2012.12.013

Statistik Burgenland. (2024). *Tourismus Jahr 2024 endgültiges Ergebnis*.

Teubner, K., Lazowski, W., & Zechmeister, T. (2022). Lake Neusiedl and Seewinkel: A hotspot area of long-term ecological research in the Danube River Basin. *Danube News*, *24*(45).

Tolotti, M., Guella, G., Herzig, A., Rodeghiero, M., Rose, N. L., Soja, G., Zechmeister, T., Yang, H., & Teubner, K. (2021). Assessing the ecological vulnerability of the shallow steppe Lake Neusiedl (Austria-Hungary) to climate-driven hydrological changes using a palaeolimnological approach. *Journal of Great Lakes Research*, *47*(5), 1327–1344. https://doi.org/10.1016/j.jglr.2021.06.004

Tóth, V. R. (2016). Reed stands during different water level periods: physico-chemical properties of the sediment and growth of Phragmites australis of Lake Balaton. *Hydrobiologia*, *778*(1), 193–207. https://doi.org/10.1007/s10750-016-2684-z

Tóth, V. R. (2025). Photosynthetic traits of Phragmites australis along an ecological gradient and developmental stages. *Frontiers in Plant Science*, *15*, 1476142.

van der Putten, W. H. (1997). Die-back of Phragmites australis in European wetlands: an overview of the European Research Programme on Reed Die-back and Progression (1993–1994). *Aquatic Botany*, *59*(3), 263–275. https://doi.org/10.1016/S0304-3770(97)00060-0

Verhoeven, J. T. A. (2014). Wetlands in Europe: Perspectives for restoration of a lost paradise. *Ecological Engineering*, *66*, 6–9. https://doi.org/10.1016/j.ecoleng.2013.03.006

Villa, P., Laini, A., Bresciani, M., & Bolpagni, R. (2013). A remote sensing approach to monitor the conservation status of lacustrine Phragmites australis beds. *Wetlands Ecology and Management*, *21*(6), 399–416. https://doi.org/10.1007/s11273-013-9311-9

Wasserportal Burgenland. (2025). *Abgestimmte Abflussdaten – Das Wehr in Mexikopuszta*. https://wasser.bgld.gv.at/hydrographie/der-neusiedler-see/webcam-wehr

Wolfram, G., Blaschke, A. P., Hainz, R., Riedler, P., & Zessner, M. (2020). *Chemische und gewässerökologische Auswir- kungen einer Dotation des Grundwassers im burgenländischen Seewinkel sowie des Neu- siedler Sees mit Wasser aus der Moson-Donau*. https://wasser.bgld.gv.at/studien/seewinkel/dotationsgutachten

Wolfram, G., Déri, L., & Zech, S. (2014). *Strategiestudie Neusiedler See – Phase 1*.

Xia, J., Shi, X., Zhou, M., Liu, S., & Deng, S. (2025). Modeling the growth dynamics of Phragmites australis with flooding stress in the Middle Yangtze River. *Ecological Modelling*, *510*. https://doi.org/10.1016/j.ecolmodel.2025.111314

Xu, T., Weng, B., Yan, D., Wang, K., Li, X., Bi, W., Li, M., Cheng, X., & Liu, Y. (2019). Wetlands of International Importance: Status, Threats, and Future Protection. *International Journal of Environmental Research and Public Health*, *16*(10), 1818. https://doi.org/10.3390/ijerph16101818

Zhao, Y., Mao, D., Zhang, D., Wang, Z., Du, B., Yan, H., Qiu, Z., Feng, K., Wang, J., & Jia, M. (2022). Mapping Phragmites australis Aboveground Biomass in the Momoge Wetland Ramsar Site Based on Sentinel-1/2 Images. *Remote Sensing*, *14*(3), 694. https://doi.org/10.3390/rs14030694

8. Supplementary materials

8.1. Ecological Definition of Clusters

To provide ecological meaning to the unsupervised clustering derived from Landsat EVI time series, a visual comparison was performed against the detailed reed classification maps produced by Csaplovics et al. (2011) and Márkus et al. (2009) for both the Austrian and Hungarian sides of the lake (Supplementary Figures 1-3).

These reference maps consisted of five principal classes of reed, ranging from Class I (vital reed) to Class V (collapsed areas). These classes were supported with additional subclasses capturing structural or transitional nuances. Our clustering was limited to five groups and could not challenge these reference maps to such a level of detail. However, the spatial overlap and functional correspondence provided a useful approximation for characterizing reed condition.

Cluster 5 and Cluster 4 aligned closely with the "vital" reed types (Classes I and II) in the reference classification, which represent dense, photosynthetically active reed stands. This cluster was characterised by the highest EVI values and strong seasonal dynamics, indicating high biomass, closed canopy cover, and vigorous regrowth patterns. It primarily included areas where reed was actively harvested, as well as dynamic reed zones along the open-lake margin. Interestingly, much of the Wulka delta appeared in Cluster 5 or Cluster 4 in our analysis. This suggest a higher functional vitality than previously mapped, where this region was largely labelled as Class III. This change likely reflects the difference in classification criteria: while the reference system emphasised structural attributes and visual appearance, our approach captured seasonal greenness patterns, approximated using EVI.

Cluster 3 aligned closely with Class III of the classification system, particularly with subclass III.A, which represent aging or structurally heterogeneous reed stands. This cluster was marked by slightly lower EVI values and more intra-annual fluctuation. It appeared to reflect reed with irregular seasonal dynamics, potentially due to structural gaps or intermixing with other plant types. Though still ecologically functional, these areas exhibited signs of early degradation or environmental stress.

Cluster 2 corresponded well to Class IV, which denotes partially degraded reed with increased openness, patchiness, or signs of transition toward non-reed vegetation. Cluster 2 captured stands with reduced EVI amplitude and lower seasonal peaks. These zones often corresponded to degraded or stressed reed, likely affected by fluctuating water levels, disturbance, or edge effects. This cluster was commonly found in interior lowland areas with a known history of disturbance.

Cluster 1 matched closely to Class V and "brown water" from the reference classification, which represents collapsed reed, water patches, and areas of ecological decline. This cluster included pixels with the lowest vegetation signal across the year, often associated with brown water areas, mudflats, or dried, collapsed reed stands. It likely captured zones where reed had failed to regrow following disturbance or where succession was progressing toward alternative land covers such as shrubs or open water. These areas represented the parts of the reed belt with the lowest vital reed.

While the match between clusters and classes was not exact, due to differences in the number of categories and the methods used, the general correspondence was strong. The comparison supported the ecological interpretability of the clusters, confirming that the unsupervised spectral-temporal groupings meaningfully reflected structural and functional differences in reed condition across the lake.

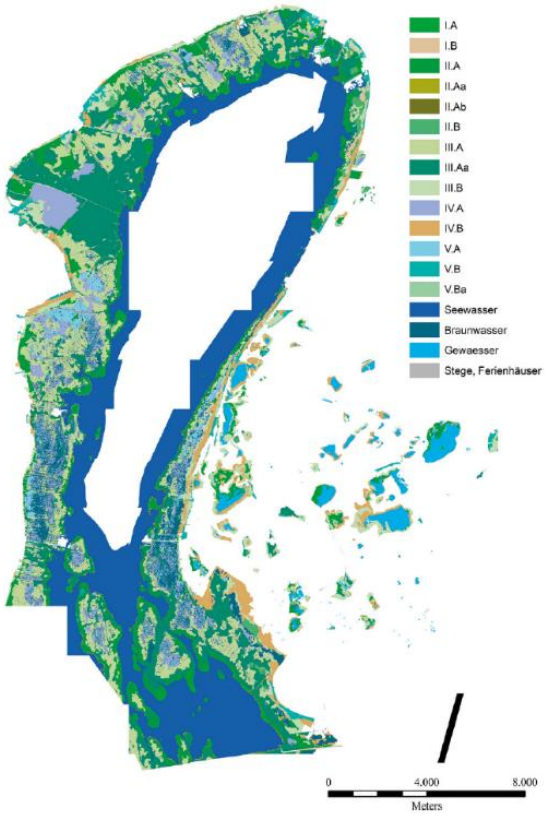

Supplementary Figure 1 Reed classification for the Austrian Part (Csaplovics & Schmidt, 2011)

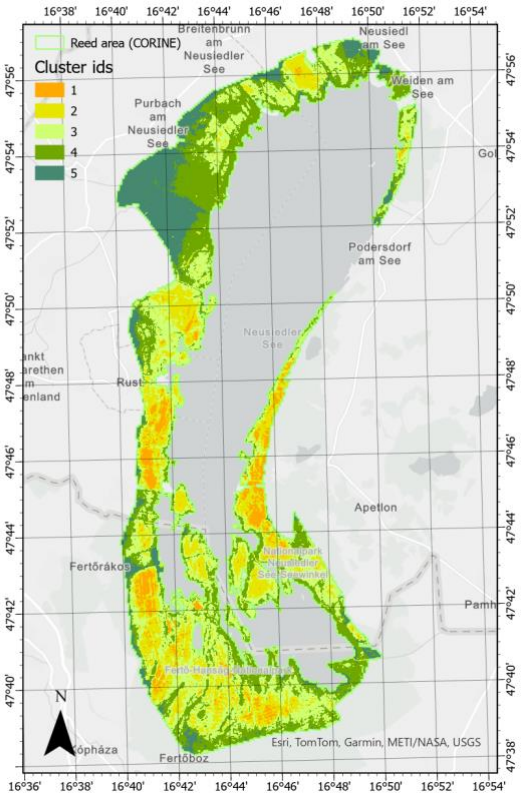

Supplementary Figure 2 Landsat 1985-2024 EVI clustering of the reed area

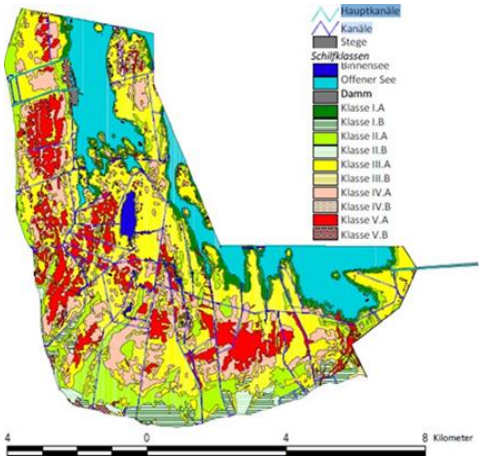

Supplementary Figure 3 Reed classification for the Hungarian part (Márkus et al., 2009)

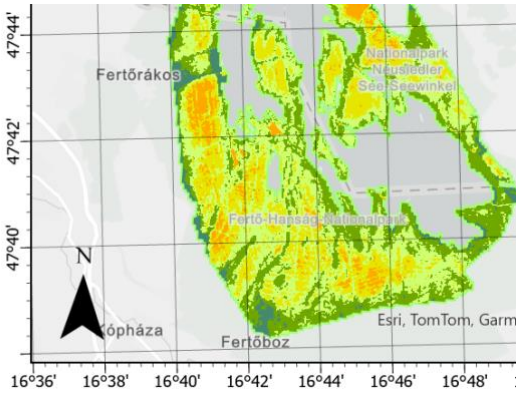

8.2. EVI time series of multi-year and single-year clustering

Supplementary Figure 4 shows the mean EVI for the 40-year period extracted for the clusters obtained with the multi-year (MY) vs per-year (SY) clustering approach. The per-year clustering is based on the k-means clustering of individual years, followed by the alignment of cluster labels across years (using the centroids of individual years/clusters) and the subsequent aggregation of EVI values for each year. Cluster 5 shows very similar trends, on the contrary, Cluster 1 presents the largest differences in the time series. The transitions from one cluster to another are mapped in the Supplementary Figure 5 along with the climatological EVI values for each cluster.

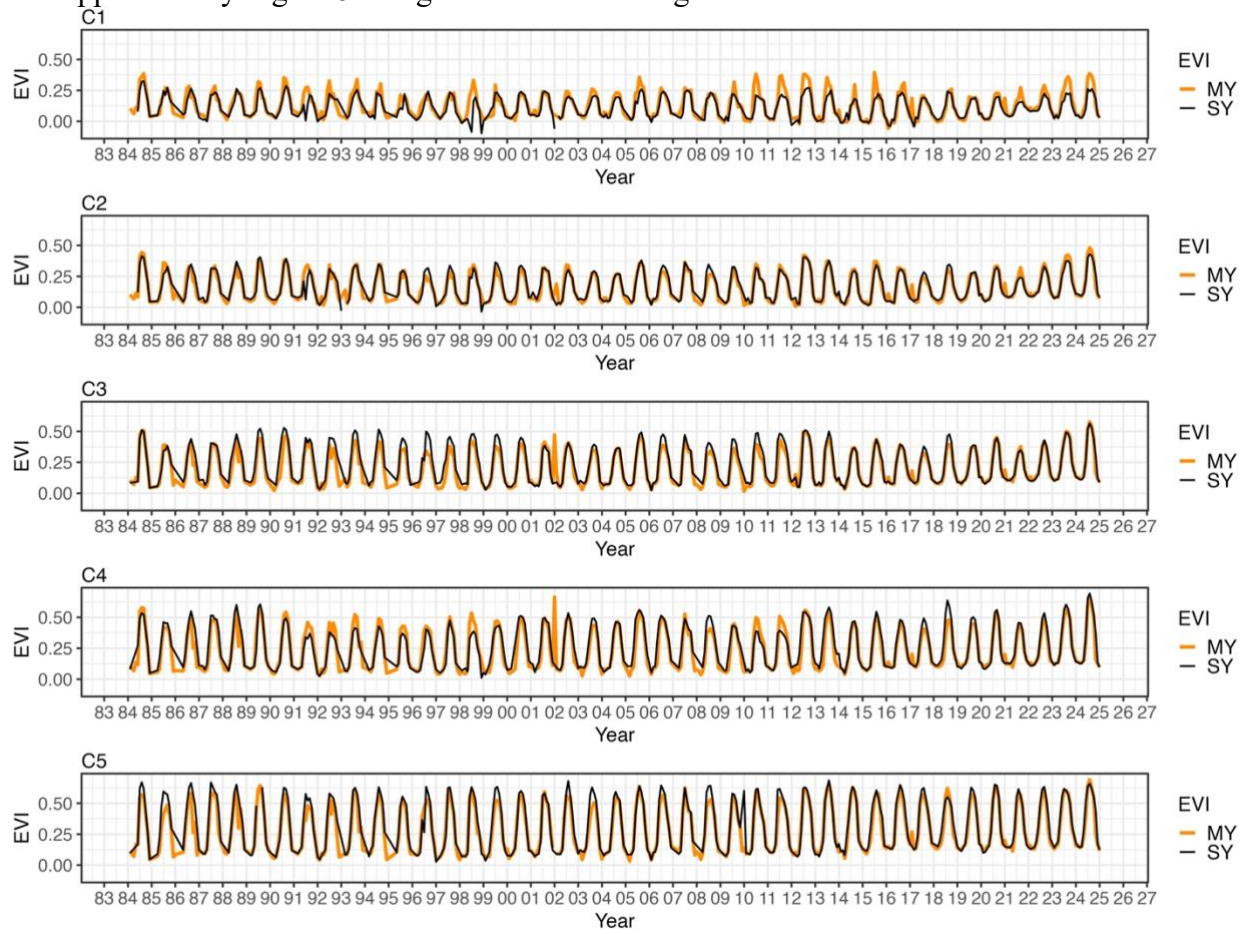

Supplementary Figure 4 Mean EVI extracted for the clusters obtained with the multi-year (MY) vs per-year (SY) clustering approach. The per-year clustering is based on the k-means clustering of individual years, followed by the alignment of cluster labels across years (using the centroids of individual years/clusters) and the subsequent aggregation of EVI values for each year.

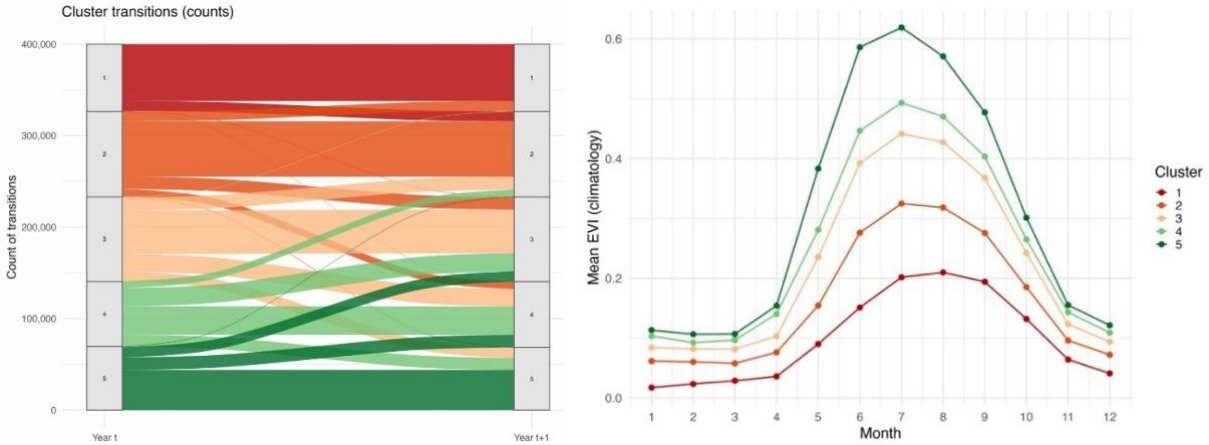

Supplementary Figure 5 Count of the transitions occurring for any year and pixel shifting cluster from year t to t+1 (left). Climatological EVI value (40-year mean) for the 5 clusters.

8.2.1. Masking of water areas and minimizing the impact of below vegetation water for the analysis of EVI

Supplementary Figure 6 show the high spatial resolution vector maps for June 2019 and for June 2022 that were used to identify the $VAWI_{log}$ values in the three categories including reed (green), water (blue) and sediment (beige). The $VAWI_{log}$ statistics are shown in the figure along with the temporal evolution of the water level (WL) from 2017 to 2026.

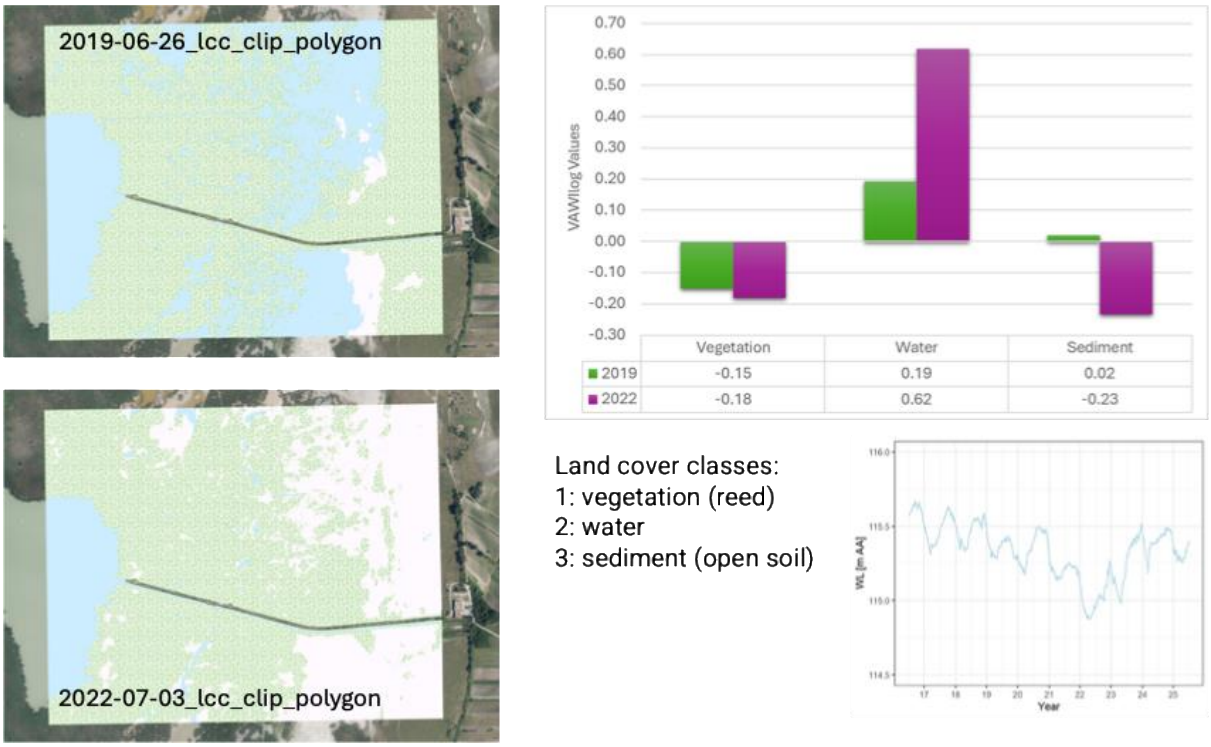

Supplementary Figure 6 Selection of the masking threshold for $VAWI_{log}$ using the land cover maps for 2019 and 2022

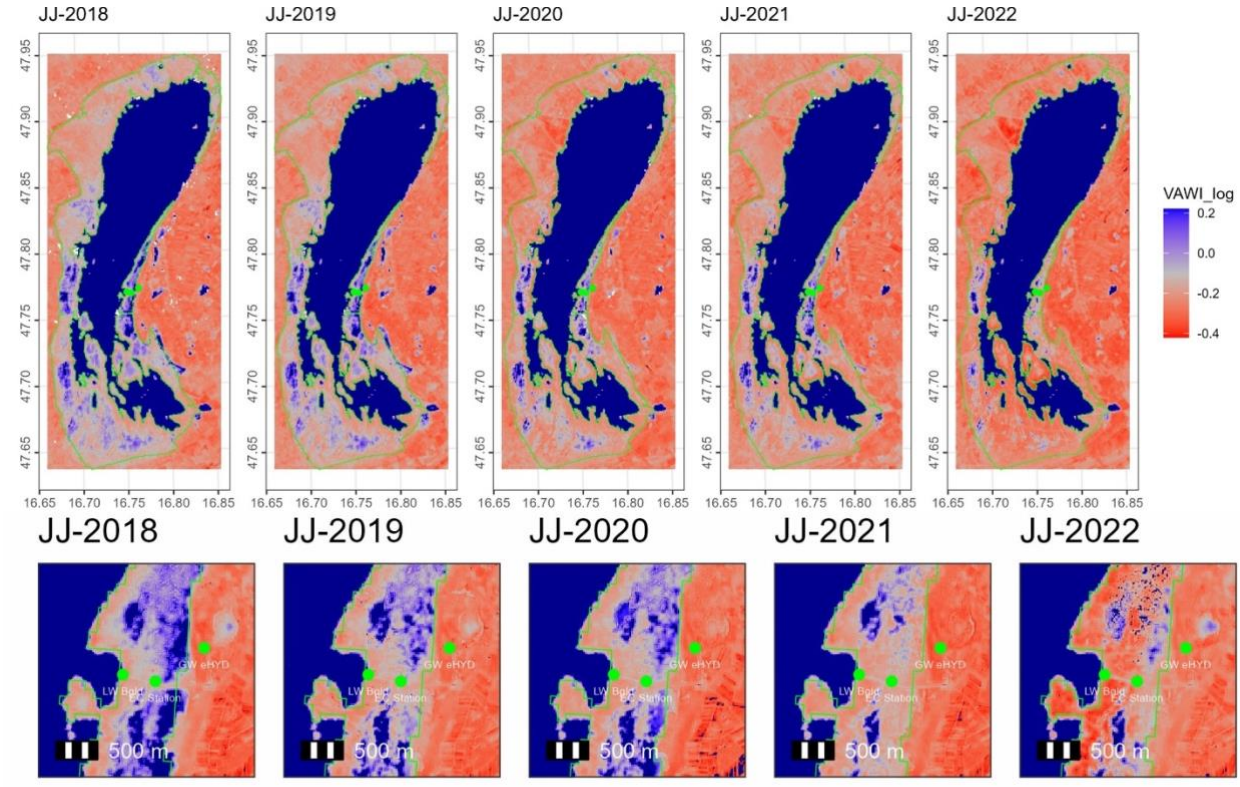

Supplementary Figure 7 Mapping of $VAWI_{log}$ in June and July from 2018 to 2022 and zoom on the biological station site.

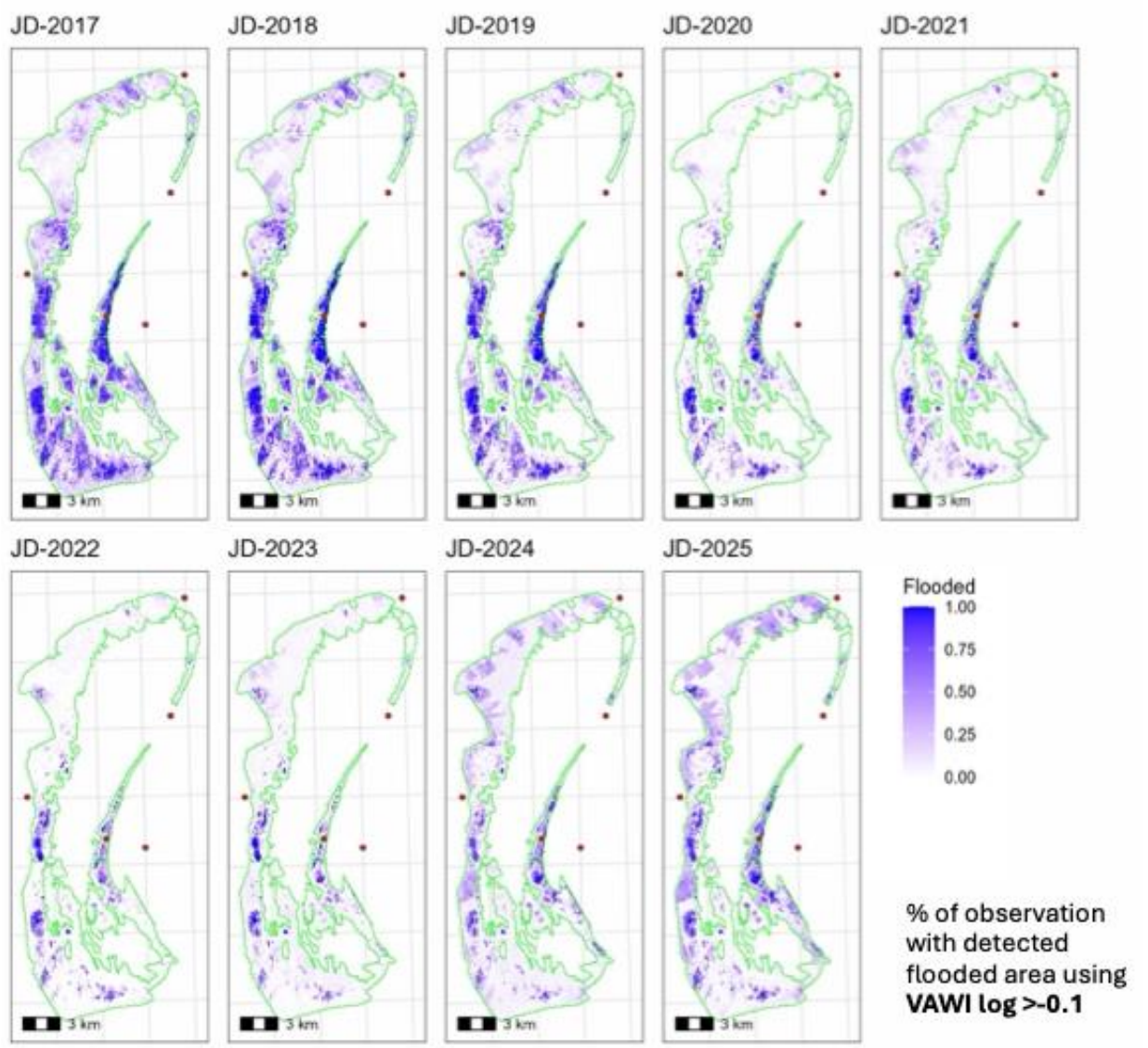

Supplementary Figure 8 Proportion of observations above threshold (VAW_{Ilog}>-0.1) from January (J) to December (D) from 2017 to 2025.

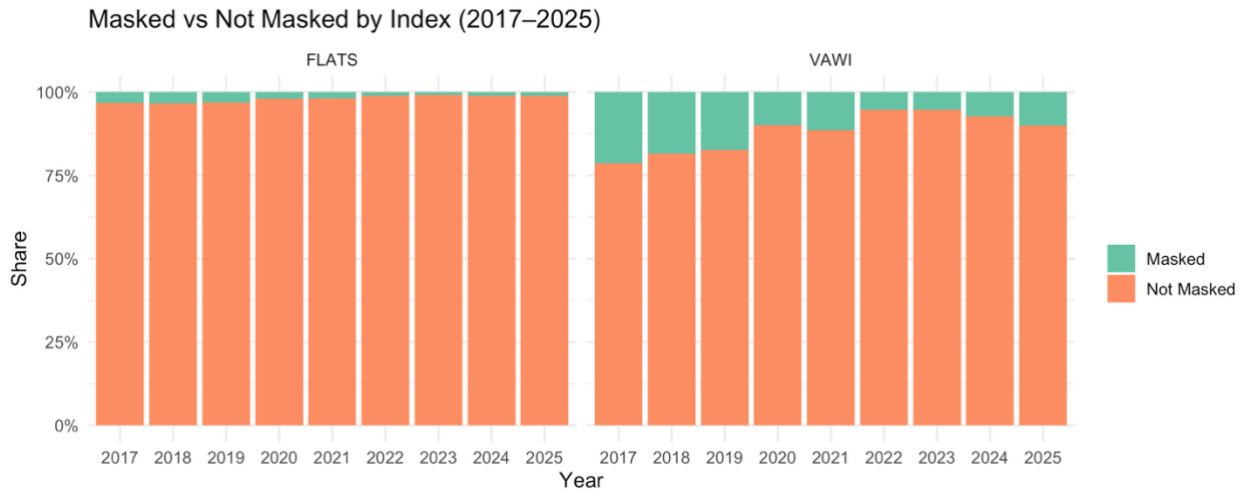

Supplementary Figure 9 Comparison of share of pixels masked for water using FLATS+ (>=0.2) and $VAWI_{log}$ (>-0.1)

8.3. Analysis of the seasonal sensitivity to surface water and air temperature

To assess the seasonal sensitivity of reed vitality to surface water level (SWL) and air temperature (AirT), we fit linear models to monthly EVI data for 1985–2025 and report the slope (β) and the significance of the correlation using the p-value, with significance evaluated at $\alpha = 0.05$. Analyses focused on the growing season (April–October), with results reported for individual months. EVI was masked using the $VAWI_{log}$ index to exclude open water and sub-canopy water, mitigating negative bias of water on EVI. Spatial heterogeneity was represented using the EVI aggregated in the five clusters (C1–C5), and correlations were estimated separately for each cluster and month. Two correlation types are discussed:

- Contemporaneous correlations: same-month EVI–SWL and EVI-AirT across years (e.g., May EVI vs. May SWL calculated using the 40 data points 1985-2025), characterizing seasonal synchrony: a positive β means higher SWL is associated with higher reed greenness/productivity in that month; a negative β suggests stress due to water logging, or reduced vigour at higher water levels.
- Lead–lag correlations: for each EVI month, correlations with SWL from antecedent and subsequent months within the same calendar year (e.g., May EVI vs. January–December SWL), quantifying antecedent and subsequent associations. Results are presented as month-by-cluster heat map that highlight the timing of the associations.

To further quantify the joint influence of thermal and water constraints on EVI, we fit a linear model with an interaction term that captures their coupling. We first removed the seasonal cycle by computing cluster- and month-specific z-score anomalies for air temperature ($AirT_{anom}$), surface water level (SWL_{anom}) using long-term monthly means and standard deviations; this centres and scales each variable and reduces seasonal confounding. For each cluster and each EVI month, we estimated the model:

$$\mathrm{EVI} = \beta_0 + \beta_T\ \mathrm{AirT} + \beta_W SWL_{anom} + \beta_{TW}\ (AirT_{anom} \times SWL_{anom}) + \varepsilon$$

where β_{TW} quantifies the strength and direction of the thermal–water interaction (positive values indicate synergistic effects; negative values indicate antagonistic effects).

8.4. Seasonal Water Sensitivity

Supplementary Figure 10 reports he strength, direction and significance of the associations between monthly SWL and cluster-specific median EVI values over 1985–2025, computed for corresponding months across years (e.g., May EVI vs. May SWL). The high-level seasonal pattern indicates that reed vitality exhibits a seasonal reversal in its association with SWL: in early spring (Month 04) EVI is negatively associated with SWL, the relationship turns positive during the peak establishment period (Month 05-06) and becomes negative again in mid–late season (Month 08-09). These associations are strongest—and often statistically significant at p-value < 0.05— in spring for degraded reeds (e.g. C1-C2) and in late summer for denser-vegetation clusters. Results are summarized in Supplementary Table 1 for each EVI month for contemporaneous and lead-lag correlations.

The differences between raw and masked EVI data are reported in Supplementary Figure 11 for C1 and C5. C1 shows the largest raw vs masked EVI differences, reflecting open-water contamination. It is therefore difficult to assess the associations between the presence/absence of water and reed vitality in this cluster using raw data. Trends seem to be similar, although the seasonal amplitude is strongly attenuated by the presence of water. C5 is not affected by the presence of water. Applying the $VAWI_{log}$ mask generally attenuates spurious negative correlations and strengthens the late-spring positive signal (May–June).

Supplementary Table 1 Results of the contemporaneous and lead-lag correlations

EVI month	Contemporaneous correlations	Lead–lag correlations
April (Month 04)	Weak negative or neutral associations, with significant values only for C2.	Weak negative associations with both antecedent and subsequent SWL for C1-C2, consistent with inundation limiting early emergence.
May–June (Months 05–06)	Shift to positive associations, however nonsignificant. Once growing season progresses, higher water levels are associated with higher EVI (beneficial moisture, reduced water stress).	Positive and significant signal spans antecedent and subsequent SWL in C2-C3 and C5, suggesting hydrologic support during rapid growth.
July–September (Months 07–09)	Predominantly neutral associations or negative from September for C4 and C5. Higher mid–late season water levels are linked to reduced canopy vigour.	Exhibits negative associations in C4-C5, consistent with inundation stress or prolonged high water lowering canopy vigour.
October (Month 10)	Mostly weakly negative/neutral, with fewer significant cases. Consistent with senescence and weaker hydrologic coupling.	

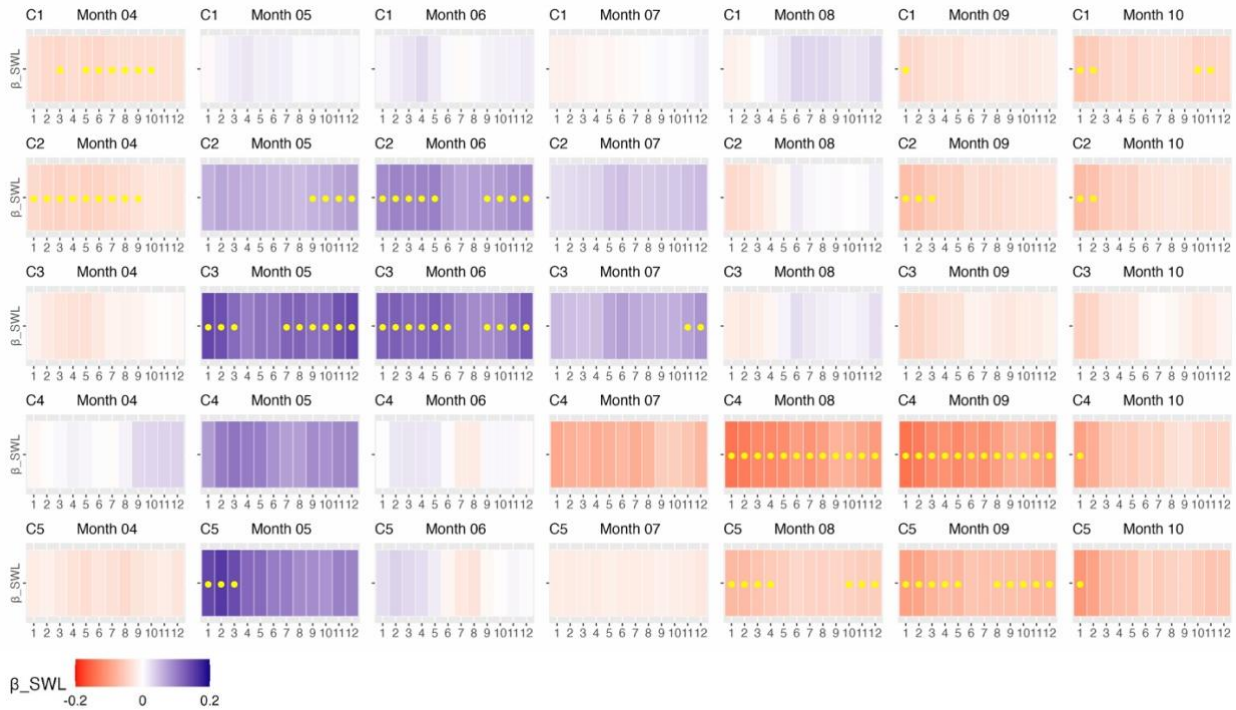

Supplementary Figure 10 Slope (β) of linear models relating monthly surface water levels (months 1–12) to cluster-specific EVI (C1–C5) for 1985–2025, restricted to April–October (months 4–10). Red indicates β<0, blue β>0. Yellow dots denote significant associations ($p<0.05$, where p is derived from the Fisher z-transformed correlation coefficient).

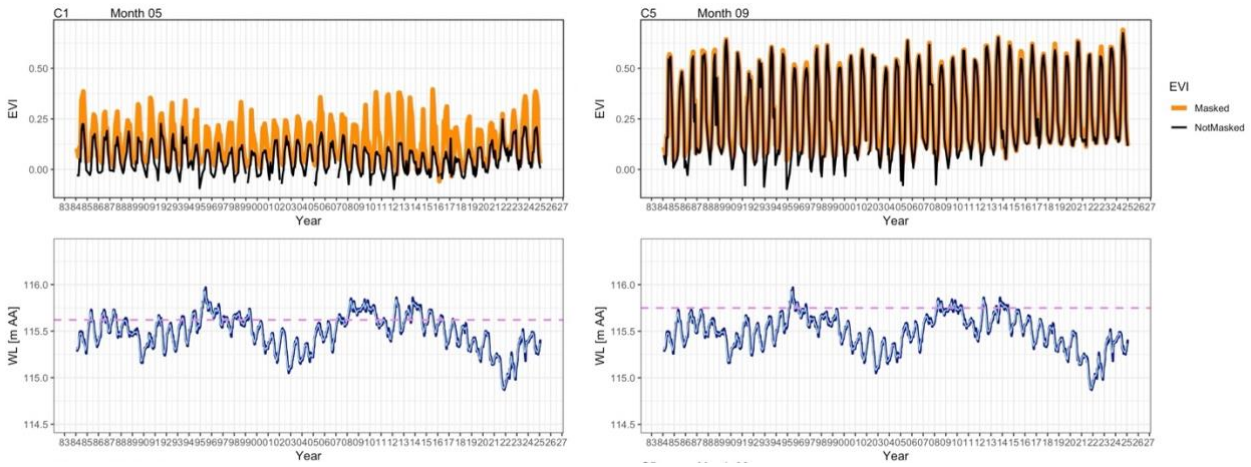

Supplementary Figure 11 Time series of EVI for Cluster 1 (top left) and Cluster 5 (top right) at Month 5 and Month 9, respectively. Orange lines denote masked EVI; black lines unmasked values. The low panels show Water Level (m a.s.l.); violet dashed lines indicate mean cluster elevation.

8.5. Effect of Air Temperature

Supplementary Figure 12 reports the correlation analysis between monthly mean air temperature and EVI values across clusters. Results show more variable and less consistent patterns than those observed for water levels. Temperature–EVI correlations show predominantly neutral or positive values across clusters, with significant cases—especially in C2–C5 potentially indicating that warmer conditions promote reed leaf-out and early canopy development. By looking at the lead–lag structure, spring antecedent shows the strongest signals - temperatures (roughly March–May) positively related to May–June EVI. This supports the idea that pre-season warmth accelerates emergence and early growth. In the late-season, positive associations suggest that warmer conditions may maintain greenness slightly longer, but effects are modest and rarely significant.

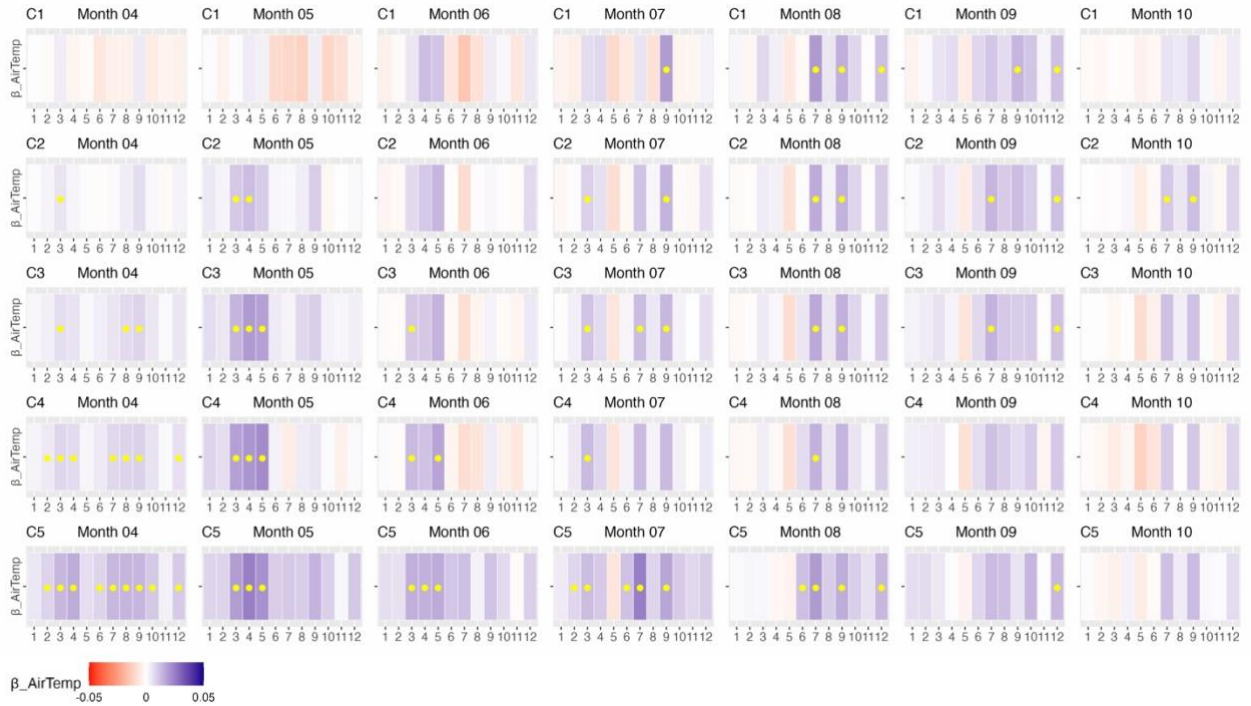

Supplementary Figure 12 Slope (β) of linear models relating monthly Air Temperatures (months 1–12) to cluster-specific EVI (C1–C5) for 1985–2025, restricted to April–October (months 4–10). Red indicates β<0, blue β>0. Yellow dots denote significant associations (p<0.05, where p is derived from the Fisher z-transformed correlation coefficient).

8.6. Interaction Air Temperature and Water Level

Only the contemporaneous associations (same month) are reported. The results confirm the trends already observed with the analysis of SWL and AirT performed individually and without seasonal normalisation. Supplementary Figure 13 shows that a weakly positive $T_{anom} \times W_{anom}$ interaction ($\beta_{TW} > 0$) is present in May-June (establishment/rapid growth) suggesting that warmth typically accelerates leaf-out and growth, but only if water is available. A strong and significant interaction is visible for C1 in July. On the contrary, a negative and significant interaction ($\beta_{TW} < 0$) is observed in September and October (late season/senescence) meaning that warmth helps less (or hurts more) when it is wet—consistent with late-season inundation making warming less beneficial.

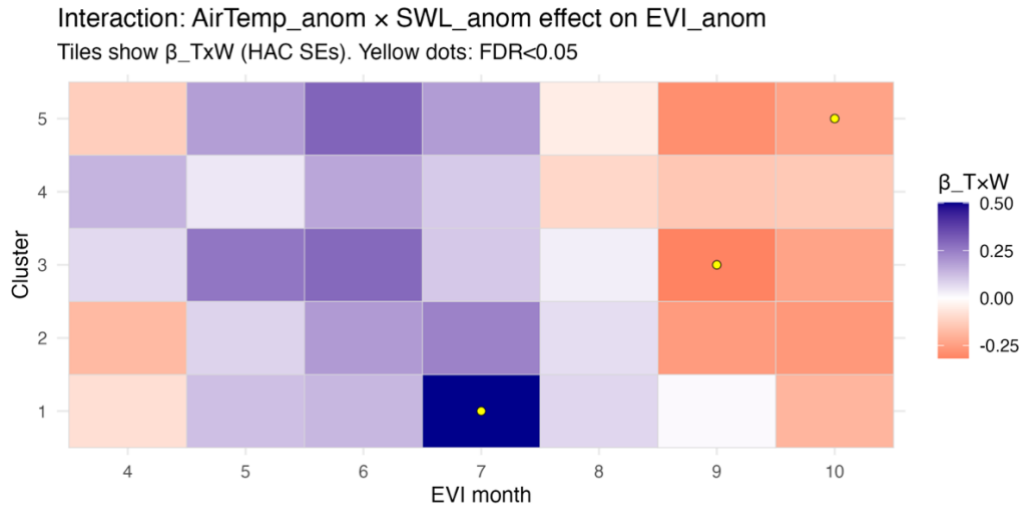

Supplementary Figure 13 Variation of the β_TW term for the Air Temperature (AirT) and Surface Water Level (SWL) interactions by EVI month (April-October) and Cluster (1-5). Only contemporaneous associations are considered here.

8.7. Impact of seasonal water fluctuations

Seasonal and extreme fluctuations in lake water levels appeared to be driving the reed productivity in Lake Neusiedl. Flood/drought regime, in particular its duration and intensity are widely recognised as the dominant environmental driver shaping wetland vegetation patterns and productivity (Xia et al. 2025). In the seasonal analysis, we found predominantly negative and significant associations between EVI and water levels from early spring and late summer. Under such anoxic conditions, litter decomposition slows and oxygen transport through rhizomes becomes restricted, reducing vigour (Bedford 2005). Comparable effects of early-season waterlogging on reed growth have also been measured in other European wetlands (Bedford 2005; Gaberščik et al. 2020; Ojdanič et al. 2023). Anoxic stress and limited gas exchange have long been recognised as major constraints on the vitality of *Phragmites australis* (van der Putten 1997). By contrast, higher water levels and warmer temperatures are associated with increased canopy vigour in May–June, when vegetation growth peaks. This indicates that during this phenological phase, additional moisture and reduced water stress are beneficial to canopy development.